THIS REPORT HAS BEEN DELIMITED

AND CLEARED FOR PUBLIC RELEASE

UNDER DOD DIRECTIVE 5200.20 AND

NO RESTRICTIONS ARE IMPOSED UPON

ITS USE AND DISCLOSURE.

DISTRIBUTION STATEMENT A

APPROVED FOR PUBLIC RELEASE;

DISTRIBUTION UNLIMITED.

UNCLASSIFIED

AD **405 534**

DEFENSE DOCUMENTATION CENTER

FOR

SCIENTIFIC AND TECHNICAL INFORMATION

CAMERON STATION. ALEXANDRIA. VIRGINIA

UNCLASSIFIED

405 534

Microwave Laboratory

W. W. HANSEN LABORATORIES OF PHYSICS

STANFORD UNIVERSITY · STANFORD, CALIFORNIA

Microwave Laboratory
W. W. Hansen Laboratories of Physics
Stanford University
Stanford, California

NONLINEAR EFFECTS IN LONGITUDINAL

ELECTRON-STREAM SLOW-WAVEGUIDE SYSTEMS

By

G. C. Van Hoven

M. L. Report No. 1026

Technical Report
April 1963

405534

ABSTRACT

This monograph presents an experimental demonstration of two heretofore unobserved nonlinear effects in systems supporting space-charge waves. The discussion is based on a physical theory which exhibits second-order coupling of these waves to those supported by an external circuit. ~~This new interaction makes possible the control of idler harmonic dispersion and, thus, removes a major obstacle to the design of a successful parametric amplifier using space-charge waves. The most important prediction of this theory is the possibility, which has been verified, of removing negative energy kinetic excitation from the slow space-charge wave.~~

The physical theory, a perturbation analysis in displacement variables, describes all possible second-order nonlinear interactions. ~~A small-signal power theorem, applicable to three frequency excitation, is derived from the dynamical equations. The conditions, restricting the location of higher idler harmonics, under which this simplification is justified are discussed.~~

The model is further specialized to the empirically valid case of a two-mode, circuit-to-stream wave interaction. ~~A quasi-linear coupled mode analysis is then developed which takes account of the kinematics of multi-frequency, multiple-mode, propagation. A general criterion for predicting the result of an arbitrary parametric coupling is given.~~

An experimental coupler, designed to test these principles, is described. ~~The character of the interactions and their placement on the dispersion diagram are shown to agree with the predictions. Parametric reverse wave amplification and, at higher coupling levels, spontaneous oscillation have been observed. A demonstration of parametric refrigeration, the transferral of negative energy excitation from the stream to the circuit, is described.~~

The low-noise amplification possibilities of devices using these principles and several problems connected with the pumping modulation are discussed. Finally, a number of alternative configurations are proposed, including a new class of fast-wave amplifiers.

- iii -

ACKNOWLEDGMENTS

To B. H. V. H.

Forsan et haec olim meminisse iuvabit.

TABLE OF CONTENTS

LIST OF FIGURES

CHAPTER I

INTRODUCTION

The invention of the klystron (Varian and Varian, 1939) and, subsequently, of the traveling-wave amplifier (Kompfner, 1946) expanded the available communications spectrum by two orders of magnitude. The low noise possibilities of these linear beam devices were realized very early (Pierce, 1950) but attempts at an effective theory were hampered by the restrictions of a ballistic interaction model and an unclear understanding of the high frequency noise excitation properties of a thermionic diode.

In the early part of the last decade two developments appeared which enabled the analysis to obtain a firm footing. The cogency of the space-charge wave theory of Hahn (1939) was rediscovered and resulted, among other things, in the derivation of a power theorem (L. J. Chu, 1951) describing linear beam interactions. Simultaneously, the work of Schottky (1918), Rack (1938), and Llewellyn and Peterson (1944) was adduced to provide a generally accepted model for the noise output at the potential minimum (Watkins, 1951; Robinson, 1952). Starting from these bases and stimulated by the development of a viable transmission line model for an accelerated electron stream (Bloom and Peter, 1954), a great number of "Minimum Noise Figure" theorems were proved and published. This series ended with the definitive work of Haus and Robinson (1955) and their statement, "The minimum noise figure of any amplifier... in which an electron beam interacts with longitudinal rf fields...is identical with that found...for the traveling-wave tube and is entirely determined by the [input] noise parameters of the beam."

This result seemed to eliminate from consideration any improved beam coupling mechanism and focused attention almost exclusively on the possibility of reducing beam noise near the potential minimum. Analyses of this region (Whinnery, 1954; Siegman, et al., 1957) have proved formidable, but they did indicate that great improvements could be obtained through

an increase in noise correlation. Indeed, subsequent experimental efforts, involving the creation of peculiar and extensive low voltage drift regions, have surpassed the theoretical predictions. These developments, culminating in the work of Currie and Forster (1959), now appear to have reached a plateau from which future progress will be slow and difficult (Wade, 1961).

The central obstacle to any interaction mechanism for lowering the noise figure limit clearly lay in L. J. Chu's kinetic power theorem (1951) and for this reason it deserves some discussion. The existence of space-charge waves on electron streams had been recognized for many years (Hahn, 1939), but the derivation of this theorem produced for the first time expressions for the small signal power carried by these waves. By using the linearized equations, Chu was able to prove that the sum of the kinetic and electromagnetic powers in a first order interaction was axially constant. In particular, he showed that the slow space-charge wave carried negative kinetic power relative to a stationary observer; thus, in the simplest case, an external waveguide need only present an energy-robbing, or lossy, impedance component to increase the amplitude of the slow wave and produce gain. This concept, along with the theory of coupled modes (Pierce, 1954), contributed greatly to an understanding of the gain mechanism in traveling-wave amplifiers.

Unfortunately, the negative energy property restricted the noise performance of devices using the slow wave. To remove excitation from this wave, a positive energy cancellation (annihilation) signal must be applied. Such cancellation is possible for the coherent signal content but not for any incoherent, or noise, content. This is the physical basis for the theoretical minimum set on the noise performance of direct coupled amplifiers using the slow space-charge wave.

For a period after the proof of this theorem, the "direct coupled" qualification was overlooked and it was believed impossible to remove slow wave noise by any means. To bypass the strictures of this theorem, various investigators chose to drop the slow wave. Excitation, coherent or incoherent, can be easily removed from the (positive energy) fast space-charge wave by direct coupled means. The problem then is to use the noise-free fast beam wave to provide amplification. The mechanism used has been long known and is called parametric coupling or, more

- 2 -

completely and clearly, nonlinear coupling by a periodic variation of parameters. The fast space-charge wave amplifier, conceived by Louisell and Quate (1958), is an application of this principle to longitudinal electron streams. Parametric coupling is provided by the impression of a strong traveling modulation or "pumping" of the electron density. This modulation impresses a spatial-temporal (propagating) periodicity on the system which forces any excitation to be carried by a series of spatial-temporal harmonics. This requirement is a generalization of Floquet's theorem describing propagation in a periodic medium (Brillouin, 1946; Mueller, 1960). These harmonics of a quiescent mode of the system have been called "idlers" and they are coupled to other modes or to other idlers by nonlinear terms in the dynamical equations. Ideally, the pump wave is designed so that the strongest coupling is that between the fast wave and its lowest order idler, an interaction producing exponential gain. Unfortunately, this aspect of the model proved to be an oversimplification. Experiments soon showed that gain was produced but that the interaction was extremely complicated, due to the lack-of space-charge wave dispersion, and involved a number of higher idlers (Ashkin, et al., 1959). The down-conversion of excitation from these frequencies effectively eliminated the noise advantages of this method of amplification.

During this period the fast wave principle was successfully applied to the design of amplifiers using the more dispersive cyclotron waves (Adler, et al., 1959). The noise performance of these amplifiers has been spectacular (Wade, 1961) but their frequency coverage is restricted by magnetic field limitations. Interestingly enough, the fast wave amplification of both of these devices depends on a dynamical model which is more general than that of Chu. The (parametric) power theorem applicable to this new model was originally developed, in another connection, by Manley and Rowe (1956) and only later applied to electron beams (Haus, 1959; Sturrock, 1961).

The realization that this new power theorem struck at the foundation of the minimum noise figure theorem was made by Sturrock (1959). He proposed a noise reduction and signal amplification configuration which retained the eminently useful, negative energy, slow wave. In this system, the exact reverse of the parametric amplification scheme is used.

The noisy electron beam first enters a traveling-wave circuit which would normally provide amplification. As in the fast wave amplifier, parametric pump excitation is introduced which changes the character of the interaction. As predicted by the parametric power theorem, signal excitation on the circuit and noise excitation on the slow wave are passively exchanged (Sturrock, 1960c), a process called "parametric refrigeration." The electron stream, now possessing a noise-free slow wave, is then used in a conventional traveling-wave interaction to produce gain.

Two early investigations of the principle of parametric refrigeration concentrated on a version using space-charge waves exclusively. An analytical treatment (Forster, 1960), using a somewhat restrictive pump wave model, predicted that the refrigeration interaction would be insensitive to higher idlers. Unfortunately, the experiments of Monson (1960) which used this configuration were unsuccessful. He again, gave insufficient space-charge wave dispersion as the reason.

The theory and experiment which we will describe relate to the circuit coupled version of the parametric refrigerator (Sturrock, 1960c). The scope will be wider than this statement would indicate in that it will attempt a general treatment of nonlinear coupling in linear beam devices. In particular, it will give a physical theory and experimental verification of a new phenomenon, parametric interaction between circuit waves and space-charge waves. The importance of this type of coupling lies in the ability to control dispersion and to inhibit unwanted idler interactions. Since the only reason for using these relatively complicated coupling means is the subversion of the minimum noise figure theorem, our attention will eventually be centered on the subclass of slow wave, or parametric refrigeration, interactions. A plan of the exposition is described below.

In Chapter II, a model is developed for an electron stream enclosed in a slow waveguide. Nonlinear dynamical equations are derived which cover all possible coupling mechanisms. These equations are couched in displacement, or polarization, variables (Bobroff, 1959; Sturrock, 1960d) which have the advantage that all cross-coupling appears in the driving terms. In addition, these variables exhibit nonlinear circuit coupling directly, a possibility which is not clear in the common Eulerian

analysis (Forster, 1960). Several applications of this theory are given, by way of example.

In Chapter III, a three frequency kinetic power theorem is derived from the nonlinear equations. Several specializations of its form are described.

In Chapter IV, a quasi-linearized two mode coupling theory and the physical assumptions necessary for its applicability are developed. Spurious idler interactions are discussed in the context of the present experiment and of previous unsuccessful experiments.

In Chapter V, the design of a circuit pumped coupler to test the two mode theory is described. Parametric coupling to circuit waves is directly demonstrated and the large space-charge assumption, used in the theory, is experimentally justified.

The first experimental observation of ideal, single idler, fast space-charge wave amplification is described. This interaction, similar to that in a backward wave amplifier, is shown to exhibit spontaneous oscillation at higher coupling levels. Finally, the parametric refrigeration interaction is verified. This verification is, in a sense, indirect since the noise-free slow wave has not been used in an amplifier, but the net of theoretical and empirical evidence shown in this paper allows no other interpretation.

In Chapter VI, the experimental results are evaluated in their required frame of reference: their use to provide low noise amplification. Several practical problems concerning the pumping modulation are discussed. Finally, a number of alternative configurations are proposed which are advantageous in respect to noise performance, bandwidth, or pump efficiency. In addition, a new class of fast wave parametric amplifiers is described.

CHAPTER II

PHYSICAL THEORY

Two indispensable aids to the understanding of a wave interaction system are the relevant power theorem and a generalized coupled mode theory (Pierce, 1954; Sturrock, 1958b). These results are often conjectured from general principles and used in the prediction of new effects, but their applicability must eventually be proved from the physical equations. We will derive these equations in this chapter, thus providing a basis for the more general considerations which follow.

In order to bring out the physical principles involved in the non-linear coupling of stream waves to circuit waves we will analyze the model commonly used in traveling-wave amplifier theory. We will visualize a cylindrical electron stream directed along the axis of a slow wave-guide. The most frequently used example is the helix which supports slow electromagnetic waves with strong longitudinal electric fields. We will assume that the beam is constrained by a very large axial magnetic field. This condition, which held in our experiments, effectively eliminates any transverse rf motions of the electrons. In addition, the beam radius is held to be considerably smaller than the circuit radius so that any variation of the dynamical variables over the beam cross section is negligible. These assumptions are those which are commonly made in longi-tudinal beam theory (Pierce, 1950) and, if certain phenomenological constants are experimentally evaluated, they have given reliable results.

Having made these assumptions, we must choose a suitable coordinate system in which to express the electron motion. The common choice of the field-like Eulerian variables leads to difficulties, however. At first glance they do not appear to predict nonlinear small-signal coupling between beam and circuit waves (Forster, 1960). In these variables this may be shown only by means of a re-expansion in terms of the force fields (Kino, 1960) or by a renormalization in terms of the direct-coupled modes

- 6 -

(Bobroff, 1960). For their directness and clarity in this respect, we will use displacement or polarization variables (Bobroff, 1959; Sturrock, 1960d). In these variables an electron in a large z-directed magnetic field changes its position, $z_0(t) \rightarrow z_0(t) + \tilde{z}(z_0,t)$, under the influence of a perturbing electric field, $\tilde{E}(z_0,t)$. The laws which relate the response to the perturbation (Bobroff, 1959; E. L. Chu, 1960a) are the velocity equation,

$$\left(\frac{\partial}{\partial t} + u_0 \frac{\partial}{\partial z_0} \right) \tilde{z}(z_0,t) = \tilde{v}(z_0,t) , \qquad (1)$$

and the Lorentz force equation,

$$\left(\frac{\partial}{\partial t} + u_0 \frac{\partial}{\partial z_0} \right) \tilde{v}(z_0,t) = - \eta \, \tilde{E}(z_0 + \tilde{z},t) , \qquad (2)$$

wherein u_0 is the axial dc velocity of the electron stream, all quantities capped by the tilde are considered to be of small amplitude, and all variables are understood to be the z-components of the corresponding vectors. At each instant in time the electric field may be expanded in a Taylor series,

$$\tilde{E}(z_0 + \tilde{z},t) = \tilde{E}(z_0,t) + \tilde{z}(z_0,t) \frac{\partial}{\partial z_0} \tilde{E}(z_0,t) + \dots ,$$

around $z = z_0$. At this point, since we have introduced a nonlinear term into the equation, it is necessary to be more specific about the time variation which will be allowed. We will assume that there are three noncommensurable excitation frequencies which, for a significant interaction to occur, must satisfy the relation

$$\omega_d = \omega_1 + \omega_2 , \qquad (3)$$

- 7 -

where all frequencies are positive. We will comment later on the conditions under which this three frequency analysis gives a valid description of a physical system.

In this model, all real physical variables are to be expanded in the form

$$
\tilde{z}(z_0, t) = \frac{1}{2}\left\{ \tilde{z}_1(z_0)e^{j\omega_1 t} + \tilde{z}_1^*(z_0)e^{-j\omega_1 t} \right.
$$
$$
\left. + \tilde{z}_2(z_0)e^{j\omega_2 t} + \tilde{z}_2^* e^{-j\omega_2 t} + \tilde{z}_d(z_0)e^{j\omega_d t} + \tilde{z}_d^* e^{-j\omega_d t} \right\} , \quad (4)
$$

where $\tilde{z}_1$, $\tilde{z}_2$ have complex amplitudes. Thus, with identifications similar to (4), the ω_1 component of the electric field may be written

$$
\tilde{E}_1(z_0 + \tilde{z}) \approx \tilde{E}_1(z_0) + \frac{1}{2}\tilde{z}_2^* \frac{\partial}{\partial z_0}\tilde{E}_d(z_0) + \tilde{z}_d \frac{\partial}{\partial z_0}\tilde{E}_2^*(z_0) ,
$$

correct to second order in small variables.

The field at z_0, at each frequency ω_i, is composed of two parts: the applied circuit field $E_{ci}(z_0)$, and the space-charge repulsion field $\tilde{E}_{si}(z_0)$. The latter, which is due to the perturbation of the electron density, may be found from Poisson's equation as we show in Appendix A. At frequency ω_1 it has the approximate form

$$
\tilde{E}_{s1}(z_0) \approx -\frac{1}{\epsilon_0}\rho_0 R_1^2 \left[\tilde{z}(z_0) - \tilde{z}(z_0)\frac{\partial}{\partial z_0}\tilde{z}(z_0) \right]_1
$$
$$
= \frac{R_1^2 \omega_p^2}{\eta}\left\{ \tilde{z}_1(z_0) - \frac{1}{2}\tilde{z}_2^* \frac{\partial}{\partial z_0}\tilde{z}_d(z_0) - \frac{1}{2}\tilde{z}_d \frac{\partial}{\partial z_0}\tilde{z}_2^*(z_0) \right\} , \quad (5)
$$

correct to second order in small variables. The phenomenological constant R_1, called the space-charge reduction factor (Branch and Mihran, 1955)

at wave number β_1 , accounts for the diminution of charge repulsion in finite geometries. The rf charge density, $\delta_1'(z_0)$, has been expressed to second order in the displacement variable through the use of the Lagrange expansion and the differential continuity condition (E. L. Chu, 1960b; Sturrock, 1960d). This calculation is shown in Appendix A. The symbols $\rho_0 < 0$ and $\omega_p^2 \equiv -\eta \rho_0/\epsilon_0$ signify the dc electron charge density and plasma frequency, respectively.

If we substitute the circuit fields and space-charge fields into the Taylor expansion, we may finally write the force equation at frequency ω_1 in the following form:

$$u_0 \left(\frac{\partial}{\partial z_0} + j\beta_{el} \right) \tilde{v}_1 = -\left\{ \eta \tilde{E}_{c1} + R_1^2 \omega_p^2 \tilde{z}_1 \right\}$$

$$- \frac{1}{2} \tilde{z}_2^* \frac{\partial}{\partial z_0} \left\{ \eta \tilde{E}_{cd} + \omega_p^2 (R_d^2 - R_1^2) \tilde{z}_d \right\}$$

$$- \frac{1}{2} \tilde{z}_d \frac{\partial}{\partial z_0} \left\{ \eta \tilde{E}_{c2}^* + \omega_p^2 (R_2^2 - R_1^2) \tilde{z}_2^* \right\} \quad , \quad (6)$$

correct to second order in small signal variables. In this expression $\beta_{el} \equiv \omega_1/u_0$ is the electronic wave number. An evident advantage of this formulation in displacement variables is that all nonlinear terms appear in the right hand or driving member of the physical equations. No re-normalization is required to produce this useful form. The only restriction to its generality is caused by the introduction of the plasma frequency reduction factor by (5) which is valid, strictly speaking, only when each term of the equation has the same wave number (see Appendix A). This applies only in the case of space-charge to space-charge coupling.

When all of the driving terms except the linear space-charge field are ignored (as in a conducting pipe with simple harmonic excitation at frequency ω_1), the "normal mode" solution of Eqs. (1) and (6) is given

in complex form by

$$\widetilde{z}_1(z_0,t) = \widehat{Z}_1 \exp\left\{ j\omega_1 t - j\left(\frac{\omega_1 \mp R_1\omega_p}{u_0}\right)z_0 \right\} , \qquad (7)$$

the well known fast/slow space-charge waves (Hahn, 1939). When the first order circuit term is included we obtain an additional solution, the "driven" wave. This solution has the dominant form (see Appendix C)

$$\widetilde{z}(z_0,t) = \eta\widehat{E}_{c1}\left[(\omega_1 - u_0\beta_{c1})^2 - R_1^2\omega_p^2\right]^{-1} e^{j(\omega_1 t - \beta_{c1}z_0)} , \qquad (8)$$

when driven by a circuit wave, $\widetilde{E}_{c1}(z_0,t) = \widehat{E}_{c1} \exp j(\omega_1 t - \beta_{c1}z_0)$.

To complete the physical description of the system the "circuit" equation, which describes the perturbation of circuit propagation due to the presence of the electron stream, must be introduced. A form which is particularly useful when the beam couples most strongly to a single circuit wave is given by Butcher (1957),

$$\left(\frac{\partial}{\partial z_0} + j\beta_{c2}\right) \widetilde{E}_{c2}(z_0) = -\frac{1}{2} \Pi_{c2}\beta_{c2}^2 K_2\sigma\widetilde{J}_2(z_0)$$

$$\approx -\frac{1}{2} \sigma\Pi_{c2}\beta_{c2}^2 K_2 \left\{ j\omega_2\rho_0\left[\widetilde{z}(z_0) - \widetilde{z}(z_0)\frac{\overset{\bullet}{\partial}}{\partial z_0}\widetilde{z}(z_0)\right]_2 \right\}$$

$$= -j\frac{1}{2} \sigma\Pi_{c2}\omega_2\beta_{c2}^2 K_2\rho_0 \left\{ \widetilde{z}_2(z_0) - \frac{1}{2}\frac{\partial}{\partial z_0}(\widetilde{z}_1^*\widetilde{z}_d) \right\} , \qquad (9)$$

where Π_{c2} is the circuit parity parameter which has the value ± 1 when $\widetilde{E}_{c2}(z_0)$ is the field of a forward/backward (group velocity and power flow) wave. We have frequency analyzed the equation explicitly so that all terms vary as $\exp(j\omega_2 t)$. The beam cross section is σ and the coupling

impedance K_2 is a positive phenomenological constant. The rf current density $\tilde{\mathfrak{J}}_2(z_0)$ has been evaluated by another form of the Lagrange expansion (A.9).

We may now assemble these equations, and their counterparts at the opposite frequencies, into the following set which describes the electron stream-circuit system correctly to second order in small quantities:

$$\left(\frac{\partial}{\partial z} + j\beta_{e1}\right)\tilde{z}_1 = \frac{\tilde{v}_1}{u_0} \tag{10}$$

$$\left(\frac{\partial}{\partial z} + j\beta_{e1}\right)\frac{\tilde{v}_1}{u_0} = -\frac{1}{2}\left\{\frac{\tilde{E}_{c1}}{V_0} + 2R_1^2\beta_p^2\tilde{z}_1\right\}$$
$$-\frac{1}{4}\tilde{z}_d\frac{\partial}{\partial z}\left\{\frac{\tilde{E}_{c2}^*}{V_0} + 2(R_2^2 - R_1^2)\beta_p^2\tilde{z}_2^*\right\}$$
$$-\frac{1}{4}\tilde{z}_2^*\frac{\partial}{\partial z}\left\{\frac{\tilde{E}_{cd}}{V_0} + 2(R_d^2 - R_1^2)\beta_p^2\tilde{z}_d\right\} \tag{11}$$

$$\left(\frac{\partial}{\partial z} + j\beta_{c1}\right)\tilde{E}_{c1} = -j\frac{1}{2}\sigma\rho_0\omega_1\Pi_{c1}\beta_{c1}^2 K_1\left\{\tilde{z}_1 - \frac{1}{2}\frac{\partial}{\partial z}(\tilde{z}_2^*\,\tilde{z}_d)\right\} \tag{12}$$

$$\left(\frac{\partial}{\partial z} - j\beta_{e2}\right)\tilde{z}_2^* = \frac{\tilde{v}_2^*}{u_0} \tag{13}$$

$$\left(\frac{\partial}{\partial z} - j\beta_{e2}\right)\frac{\tilde{v}_2^*}{u_0} = -\frac{1}{2}\left\{\frac{\tilde{E}_{c2}^*}{V_0} + 2R_2^2\beta_p^2\tilde{z}_2^*\right\}$$
$$-\frac{1}{4}\tilde{z}_d^*\frac{\partial}{\partial z}\left\{\frac{\tilde{E}_{c1}}{V_0} + 2(R_1^2 - R_2^2)\beta_p^2\tilde{z}_1\right\}$$
$$-\frac{1}{4}\tilde{z}_1\frac{\partial}{\partial z}\left\{\frac{\tilde{E}_{cd}^*}{V_0} + 2(R_d^2 - R_2^2)\beta_p^2\tilde{z}_d^*\right\} \tag{14}$$

and

$$\left(\frac{\partial}{\partial z} - j\beta_{c2}\right)\widetilde{E}^*_{c2} = j\frac{1}{2}\omega_0\Pi_{c2}\omega_2\beta^2_{c2}K_2\left\{\widetilde{z}^*_2 - \frac{1}{2}\frac{\partial}{\partial z}(\widetilde{z}_1\widetilde{z}^*_d)\right\} \quad . \quad (15)$$

The two previously undefined symbols introduced into these equations are the dc beam voltage V_0 and $\beta_p \equiv \omega_p/u_0$, the plasma wave number. These equations describe, within the approximations inherent in the model, all of the three frequency interactions possible between circuit waves and space-charge waves.

In applying them to a physical situation one is normally interested in a specific coupling, say between a circuit wave at frequency ω_1 and a space-charge wave at frequency ω_2 . For a significant cumulative interaction to be possible, there must be approximate phase velocity synchronism between the beam wave and an idler harmonic of the circuit wave. In terms of the wave numbers of the coupled modes, this requires the satisfaction of an additional relation (Tien, 1958) of the form

$$\beta_d = \beta_1 + \beta_2 + \Delta\beta \approx \beta_1 + \beta_2 \quad , \quad (16)$$

where the approximation is that $\Delta\beta/\beta_{1,2} \ll 1$. The rationale behind this condition may be seen from the equations when the specific z-dependence of the quantities

$$\widetilde{A}_1(z) = \widehat{A}_1(z)e^{-j\beta_1 z} \quad (17)$$

is inserted. For small coupling per wavelength $\widehat{A}_1(z)$ is a slowly varying amplitude

$$\left|\frac{d}{dz}\widehat{A}_1(z)\right| \ll \left|\beta_1\widehat{A}_1(z)\right| \quad , \quad (18)$$

describing the departure from the pure uncoupled mode, and the burden of the spatial dependence is borne by the wave numbers. If the approximation of (16) does not hold, one of the terms of the relevant (wave number analyzed) dynamical equations would have a rapid variation and, thus, a small average effect.

With this understanding, any application of the general equations to a physical problem results in the omission of those terms whose wave numbers fail to satisfy (16). The remaining terms are characterized by a single value of the uncoupled wave number for each frequency (as we have mentioned, this is inherent in the model in the special case of nonlinear space-charge to space-charge coupling).

In any application, the partial derivatives remaining in the <u>driving</u> terms of the equations are eliminated by the use of relation (18) to set

$$\tilde{A}_j^*(z) \frac{\partial}{\partial z} \tilde{A}_1(z) = \tilde{A}_j^*(z) e^{-j\beta_1 z} \left(\frac{d}{dz} - j\beta_1\right) \hat{A}_1(z)$$

$$\cong - j\beta_1 \tilde{A}_j^*(z) \tilde{A}_1(z) \quad . \tag{19}$$

Since these derivatives only occur in terms which are already of second degree in small variables, the order of the analysis is not upset.

We have not written the third set of equations for quantities varying as ω_d since we will eventually assign this wave the role of the nearly constant, large amplitude, pump wave.

We will now discuss several applications of these equations:

(a) Traveling-Wave Amplifier.

If there is no excitation at ω_d , the nonlinear terms disappear and we are left with the equations describing direct-coupled interactions of the traveling-wave type. Assuming a solution of the form of (17), we may combine (10) and (11) into the electronic equation of traveling-wave tube theory (Pierce, 1950):

$$\left[\left\{ (\beta - \beta_c)^2 - R^2\beta_p^2 \right\} \hat{Z} - \frac{1}{2} \frac{\hat{E}_c}{V_0} = 0 \right. ,$$

where we have dropped the frequency subscripts. Similarly (12), the circuit equation, may be written in the form

$$- \frac{1}{2} \Pi_c \beta_e \beta_c^2 \sigma u_0 \rho_0 K \hat{Z} + (\beta - \beta_c) \hat{E}_c = 0 \quad .$$

The Cramer determinant of this system of equations gives the well-known dispersion relation of the traveling-wave tube (Hutter, 1960):

$$(\beta - \beta_c) \left\{ (\beta - \beta_e)^2 - R^2 \beta_p^2 \right\} = - \Pi_c \beta_e \beta_c^2 C^3 \quad . \qquad (20)$$

We have introduced $C^3 \equiv K I_0 / 4V_0$, the beam coupling coefficient (Pierce, 1950), and the dc current $I_0 = - \sigma \rho_0 u_0$. The solutions to this equation are well known and predict amplification in forward circuit wave interactions $(\Pi_c = + 1)$ when

$$\beta_e + \beta_p \approx \beta_c \quad .$$

This condition indicates that the velocity of the slow space-charge wave is approximately equal to the velocity of the circuit wave.

(b) Fast Space-Charge Wave Parametric Amplifier

As a second application of our formalism we will develop an expression for the gain constant of the fast space-charge wave amplifier of Louisell and Quate (1958; Louisell, 1959). To conform to the model analyzed in these references, we assume that no circuit fields exist in the system and that the waves of interest in the coupling are all fast space-charge waves,

$$\beta_i = \beta_{ei} - R_i \beta_p \quad , \qquad (21)$$

including the wave which carries the pumping modulation. With these restrictions, the relevant forms of (10), (11), (13), and (14) combine

to provide

$$\left\{ \left(\frac{\partial}{\partial z} + j\beta_{e1} \right)^2 + R_1^2 \beta_p^2 \right\} \tilde{z}_1$$

$$= -\frac{1}{2} j\beta_p^2 \left\{ \beta_2 \left(R_2^2 - R_1^2 \right) - \beta_d \left(R_d^2 - R_1^2 \right) \right\} \tilde{z}_2^* \tilde{z}_d \qquad (22)$$

and

$$\left\{ \left(\frac{\partial}{\partial z} - j\beta_{e2} \right)^2 + R_2^2 \beta_p^2 \right\} \tilde{z}_2^*$$

$$= \frac{1}{2} j\beta_p^2 \left\{ \beta_1 \left(R_1^2 - R_2^2 \right) - \beta_d \left(R_d^2 - R_2^2 \right) \right\} \tilde{z}_1 \tilde{z}_d^* \quad . \qquad (23)$$

We now use the conditions (17) and (18) in expanding the left hand sides of these equations and ignore terms of order $R_1^3 \beta_p^3$ on the right to obtain

$$\frac{d}{dz} \hat{z}_1 = -\frac{1}{4} \left(j\beta_{ed} \hat{z}_d \right) R_2 \beta_p \left\{ \frac{\beta_{e1} \left(R_d^2 - R_1^2 \right) + \beta_{e2} \left(R_d^2 - R_2^2 \right)}{R_1 R_2 \left(\beta_{e1} + \beta_{e2} \right)} \right\} \hat{z}_2^* \qquad (24a)$$

$$\frac{d}{dz} \hat{z}_2^* = \frac{1}{4} \left(j\beta_{ed} \hat{z}_d^* \right) R_1 \beta_p \left\{ \frac{\beta_{e1} \left(R_d^2 - R_1^2 \right) + \beta_{e2} \left(R_d^2 - R_2^2 \right)}{R_1 R_2 \left(\beta_{e1} + \beta_{e2} \right)} \right\} \hat{z}_1 \quad . \qquad (24b)$$

In order to conform to the usage of Louisell and Quate we introduce the pump modulation index,

$$m \equiv \frac{\hat{J}_d}{J_0} = \frac{j\omega_d \rho_0 \hat{z}_d}{-\rho_0 u_0} = -j\beta_{ed} \hat{z}_d \quad , \qquad (25)$$

- 15 -

where $\hat{J}_d$ is assumed to be axially constant and is adequately expressed by the first term of the generalized Lagrange expansion (A.9). Thus, we may write

$$\left\{ \frac{d^2}{dz^2} - \frac{1}{16} |m|^2 R_1 R_2 \beta_p^2 \left[\frac{\beta_{e1}\left(R_d^2 - R_1^2\right) + \beta_{e2}\left(R_d^2 - R_2^2\right)}{R_1 R_2 \left(\beta_{e1} + \beta_{e2}\right)} \right]^2 \right\} \hat{z}_1 = 0 . \quad (26)$$

When the condition of synchronism

$$\beta_{ed} - R_d \beta_p = \beta_{e1} - R_1 \beta_p + \beta_{e2} - R_2 \beta_p$$

or

$$R_d = R_1 + R_2 ,$$

is used, and we assume that $\hat{z}_1(z)$ has the form

$$\hat{z}_1(z) = \overline{Z}_1 e^{\pm sz} ,$$

we obtain the result of Louisell (1959),

$$s = \pm \frac{1}{4} |m| \beta_p \sqrt{R_1 R_2} \left\{ 2 + \frac{R_1}{R_2} \frac{\omega_2}{\omega_d} + \frac{R_2}{R_1} \frac{\omega_1}{\omega_d} \right\} . \quad (27)$$

If, finally, the special case of degenerate operation $\omega_1 = \omega_2 = \frac{1}{2} \omega_d$ is inserted, we obtain the result

$$s = \pm \frac{3}{4} R \beta_p |m| ,$$

where $R = R_1 = R_2$ has been used. This is the form originally found by Louisell and Quate (1958), predicting exponential growth along the beam.

- 16 -

If, under the same assumptions, we had used a circuit field $\widetilde{E}_{cd}$ to provide the driving wave, we would have obtained the equations describing the "circuit pumped" fast space-charge wave amplifier (Wade and Adler, 1959).

CHAPTER III

POWER THEOREM

Now that we have developed a physical theory which can be applied
to any multiply-excited circuit wave-stream wave system, it is profitable
to see if the results that we have obtained, and those we wish to obtain,
may be found from any more general approach. We shall show that this is,
indeed, possible.

One of the more essential aids to an understanding of the interactions
which may occur in an electron stream-circuit system is the knowledge of
the relevant power theorem. The concept is an old one (L. J. Chu, 1951)
which has been extensively developed (Sturrock, 1958a; Bobroff et al.,
1962). For our purposes we shall derive a general, three frequency,
power theorem from the small signal equations which we have developed.

It was L. J. Chu (1951) who first realized that the linearized
equations describing a system could be used to derive a meaningful con-
servation relation between second order quantities. These quantities,
the "formal" energy and power, properly describe the characteristics of
the hypothetical system which satisfy the linear equations (Sturrock,
1958a; Bers and Penfield, 1962).

In the case in which we are interested, the equations (10) to (15)
are of second order in small amplitudes but they have been quasi-linearized
by the assumption that the quantities describing the driving or pump
wave, $\tilde{z}_d$ and $\tilde{E}_{cd}$, have large substantially-constant amplitudes.
Thus, we may use these equations to derive a formal second order conser-
vation relation.

To prove this theorem we need only make the stipulation, which is
customary in order to facilitate axial Fourier analysis, that the wave
numbers satisfy the addition relation (16). Since this approximation
will only be used in terms on the right hand sides of (10) to (15) which
are already of second degree in small signal variables, it does not affect
the order of the analysis. A simplification of this type appears to be

necessary in order for each term of the power theorem to apply to a single frequency. In the exact treatment of Haus (1958) the kinetic power variables contain contributions from many frequencies.

.With this understanding and the abbreviated usage of (n)* for the complex conjugate of the total equation (n), the proof may be obtained by the following formal procedure:

$$
\frac{\Pi_{c1}}{\omega_1}\,\frac{\widetilde{E}_{c1}}{2\beta_{c1}^2\,K_1}\,(12)^* \;+\; \frac{\Pi_{c1}}{\omega_1}\,\frac{\widetilde{E}_{c1}^{\;*}}{2\beta_{c1}^2\,K_1}\,(12)
$$

$$
+\, j\,\frac{I_0\,u_0}{4\eta}\left\{ \widetilde{z}_1\,(11)^* - \widetilde{z}_1^{\;*}\,(11) + \frac{\widetilde{v}_1^{\;*}}{u_0}\,(10) - \frac{\widetilde{v}_1}{u_0}\,(10)^* \right\}
$$

$$\tag{28}$$

$$
-\,\frac{\Pi_{c2}}{\omega_2}\,\frac{\widetilde{E}_{c2}}{2\beta_{c2}^2\,K_2}\,(15) \;-\; \frac{\Pi_{c2}}{\omega_2}\,\frac{\widetilde{E}_{c2}^{\;*}}{2\beta_{c2}^2\,K_2}\,(15)^*
$$

$$
-\, j\,\frac{I_0\,u_0}{4\eta}\left\{ \widetilde{z}_2\,(14) - \widetilde{z}_2^{\;*}\,(14)^* + \frac{\widetilde{v}_2^{\;*}}{u_0}\,(13)^* - \frac{\widetilde{v}_2}{u_0}\,(13) \right\} \;,
$$

where the dc condition $u_0^2 = 2\eta\,V_0$ has been used. The right hand sides of these equations and the $j\beta$ terms of the left hand sides cancel so that one is left with the following two-frequency power theorem:

•

- 19 -

$$0 = \frac{1}{\omega_1} \frac{\partial}{\partial z} \left\{ \Pi_{c1} \frac{\tilde{E}_{c1} \tilde{E}_{c1}^{*}}{2\beta_{c1}^2 K_1} + \frac{1}{8} \frac{u_0^2}{\eta} \frac{1}{Z_{01}} (\tilde{v}_1 + jR_1 \omega_p \tilde{z}_1)(\tilde{v}_1^{*} - jR_1 \omega_p \tilde{z}_1^{*}) \right.$$

$$\left. - \frac{1}{8} \frac{u_0^2}{\eta} \frac{1}{Z_{01}} (\tilde{v}_1 - jR_1 \omega_p \tilde{z}_1)(\tilde{v}_1^{*} + jR_1 \omega_p \tilde{z}_1^{*}) \right\}$$

$$- \frac{1}{\omega_2} \frac{\partial}{\partial z} \left\{ \Pi_{c2} \frac{\tilde{E}_{c2} \tilde{E}_{c2}^{*}}{2\beta_{c2}^2 K_2} + \frac{1}{8} \frac{u_0^2}{\eta} \frac{1}{Z_{02}} (\tilde{v}_2 + jR_2 \omega_p \tilde{z}_2)(\tilde{v}_2^{*} - jR_2 \omega_p \tilde{z}_2^{*}) \right.$$

$$\left. - \frac{1}{8} \frac{u_0^2}{\eta} \frac{1}{Z_{02}} (\tilde{v}_2 - jR_2 \omega_p \tilde{z}_2)(\tilde{v}_2^{*} + jR_2 \omega_p \tilde{z}_2^{*}) \right\} \qquad (29a)$$

$$= \frac{\partial}{\partial z} \left\{ \frac{\Pi_{c1}}{\omega_1} \frac{\tilde{E}_{c1} \tilde{E}_{c1}^{*}}{2\beta_{c1}^2 K_1} - \frac{\Pi_{c2}}{\omega_2} \frac{\tilde{E}_{c2} \tilde{E}_{c2}^{*}}{2\beta_{c2}^2 K_2} + j \frac{I_0 u_0}{4\eta} \left[\tilde{z}_1 \frac{\tilde{v}_1^{*}}{u_0} - \tilde{z}_1^{*} \frac{\tilde{v}_1}{u_0} \right] \right.$$

$$\left. - j \frac{I_0 u_0}{4\eta} \left[\tilde{z}_2 \frac{\tilde{v}_2^{*}}{u_0} - \tilde{z}_2^{*} \frac{\tilde{v}_2}{u_0} \right] \right\} = 0 \qquad (29b)$$

In this equation we have introduced the impedance (Bloom and Peter, 1954)

$$Z_{0i} \equiv 2 \frac{R_i \omega_p}{\omega_i} \frac{V_0}{I_0} \qquad , \qquad (30)$$

which relates space-charge propagation to that on a transmission line.

It is profitable, at this point, to introduce normalized amplitudes for the circuit and kinetic power excitation. The definitions are indicated by the form of the terms in the power theorem (29a). In the case

of the circuit excitation we set

$$\tilde{b}_{ci} = \frac{1}{\sqrt{2K_i}} \frac{\tilde{E}_{ci}}{\beta_{ci}} \qquad (31)$$

so that the circuit power is given by $P_{ci} = \Pi_{ci}\tilde{b}_{ci}\tilde{b}_{ci}^{*} \equiv \Pi_{ci}b_{ci}^{2}$, the last form being an abbreviation. The beam excitation terms require the introduction of the normalized amplitudes,

$$\tilde{a}_{1\pm} \equiv \frac{1}{2} \frac{u_0}{\eta} \frac{1}{\sqrt{2Z_{01}}} (\tilde{v}_1 \pm jR_1 \omega_p \tilde{z}_1)$$

$$(32)$$

$$= \frac{1}{2} \sqrt{\frac{\omega_1}{R_1 \omega_p}} V_0 I_0 \left(\frac{\tilde{v}_1}{u_0} \pm jR_1 \beta_p \tilde{z}_1 \right) \quad ,$$

where the plus/minus signs signify the fast/slow space-charge wave. This identification has been used previously by Bobroff and Haus (1958) and will be shown explicitly in the next section. The space-charge wave impedance, Z_{01} at frequency ω_1 (30) has been introduced for dimensional reasons and to enable the transformation of the dynamical equations into normal mode form.

Before writing the power theorem in its final form, we will make one important generalization of the three frequency system which has been described. Until now we have restricted the discussion, for the sake of showing an explicit calculation, to the case of sum frequency pumping in which $\omega_d = \omega_1 + \omega_2$. We could equally as well have treated difference frequency pumping, $\omega_d = \omega_1 - \omega_2$, in which case the only modification to the dynamical equations would be the permutation of several signs and complex conjugations. More precisely, the right hand sides of the ω_1 equations (10), (11), (12) will be changed by the replacements,

$$\tilde{z}_2 \leftrightarrow \tilde{z}_2^{*}$$

$$\beta_2 \rightarrow - \beta_2 \qquad ,$$

and the right hand sides of the ω_2 equations will be changed by

$$\tilde{z}_1 \leftrightarrow \tilde{z}_1{}^* \qquad \tilde{z}_d \leftrightarrow \tilde{z}_d{}^*$$

$$\beta_1 \rightarrow -\beta_1 \qquad \beta_d \rightarrow -\beta_d \qquad .$$

Having made these transposals, a proof similar to that given previously (28) shows that the power theorem is changed by the substitution $\omega_2 \rightarrow -\omega_2$.

As a result of this discussion it is possible to <u>define</u> a pump frequency "parity" parameter by the relations

$$\omega_d = \omega_1 + \Pi_p \, \omega_2$$

$$\beta_d \approx \beta_1 + \Pi_p \, \beta_2 \qquad .$$

(33)

Thus, Π_p has value ± 1 for sum/difference frequency pumping and all frequencies are considered to be <u>positive</u> numbers. In the special case that $\omega_d = 0$ we must have $\omega_1 = \omega_2$, or $\Pi_p = -1$.

There is one clarification which is necessary before we can meaning-fully apply the parametric power theorem. This relates to the "single wave" assumption used in the proof. By this usage <u>all</u> excitations at ω_1 are assumed to propagate with wave number β_1 . In physical situations of interest we are concerned with coupling to <u>either</u> a space-charge wave <u>or</u> to a circuit wave at ω_1 and the wave number of the one which is not desired is, by design, isolated. Thus, the theorem is to be applied separately, with different β_1's , to conditions of nonlinear space-charge to circuit wave coupling or to conditions of nonlinear space-charge to space-charge wave coupling.

With this understanding, and the mode amplitude definitions previously given, the <u>space-charge</u> to <u>space-charge</u> power balance may be expressed by (34):

$$\frac{\partial}{\partial z} \left\{ \frac{1}{\omega_1} (\tilde{a}_{1+}^2 - \tilde{a}_{1-}^2) - \Pi_p \frac{1}{\omega_2} (\tilde{a}_{2+}^2 - \tilde{a}_{2-}^2) \right\} = 0 \qquad . \quad (34)$$

The case which is of greater interest in a discussion of the parametric refrigeration interaction is that of stream wave to circuit wave coupling under large space-charge conditions. For pure fast space-charge wave excitation, (10) and (32) show that the slow wave amplitude a_{1-} vanishes. Thus, (34) indicates that we may introduce the stream wave power parity parameter $\Pi_s = \pm 1$ for large space-charge fast/slow waves. For the family of electron stream interactions which includes parametric refrigeration, the power theorem becomes

$$\frac{\partial}{\partial z} \left\{ \frac{\Pi_{c1}}{\omega_1} \tilde{b}_{c1}^2 - \Pi_p \frac{\Pi_{s2}}{\omega_2} \tilde{a}_2^2 \right\} = 0 \quad , \tag{35}$$

correct to third order in small-signal variables and perturbations in wave number. Again, it should be remembered that all frequencies are positive.

The great interest in the derivation of the small signal power theorem describing a linear or quasi-linear system is its usefulness in predicting the interactions which may occur. The other essential ingredient of this prediction is the knowledge that the system can be correctly described by a coupled mode formulation. This concept will be developed in the following chapter.

CHAPTER IV

COUPLED MODE ANALYSIS

Many systems in nature can be adequately described by linear or quasi-linear equations. In particular, the general parametric stream-circuit configuration of Chapter II conforms to this description. The desired nonlinear effects are those caused by the impression of a high-level pump wave which, in relation to the low-level signal waves, may be considered to have a substantially constant amplitude. This assumption allows a linear treatment of the second order terms in the equations. Under the common conditions of harmonic excitation and weak coupling these equations may be re-expressed in terms of the quiescent normal modes of the system with small intermode interaction coefficients. The treatment of this generalized class of dynamical equations was conceived by Pierce (1954; Gould, 1955) and is called the Coupling of Modes theory.

We will first describe this theory for a general quasi-linear coupling of two modes. Then we will show that the physical equations which we have previously derived may be put in an expansion of this form and we will discuss the assumptions required to simplify the problem to a coupling of two modes. Finally, we will explore the special problem of the linear and nonlinear couplings of space-charge and circuit waves to which (35) may be applied.

A. GENERAL QUASI-LINEAR COUPLING

In a physical system which may be adequately described by the quasi-linear coupling of two modes the dynamical equations may be put in a particularly simple form. This result, a generalization of that of Pierce (1954), indicates that the small signal mode amplitudes $\tilde{a}$ and $\tilde{b}$,

coupled by a pump wave d , satisfy the equations

$$\left\{\frac{d}{dz} + j\beta_a\right\} \tilde{a}(z) = \omega_a \kappa_{ab} \, de^{-j\beta_d z} \, \tilde{b}^*(z) \qquad (36)$$

$$\left\{\frac{d}{dz} - j\beta_b\right\} \tilde{b}^*(z) = \omega_b \kappa_{ba} \, d^* e^{j\beta_d z} \, \tilde{a}(z) \quad , \qquad (37)$$

where κ_{ab} and κ_{ba} describe the strength of the coupling. The equations
are quasi-linear by virtue of the assumption that the driving or coupling
wave amplitude, d , at $\omega_d = \omega_a + \omega_b$ is a constant.

If we assume that the system, as described by these equations,
satisfies a small signal power theorem, we will be able to obtain a con-
straint on the coupling coefficients. Let the power theorem have the
form

$$\frac{\Pi_a}{\omega_a} \frac{d}{dz} (\tilde{a}\tilde{a}^*) - \frac{\Pi_b}{\omega_b} \frac{d}{dz} (\tilde{b}\tilde{b}^*) = 0 \quad , \qquad (38)$$

where Π_a and Π_b are power parity parameters. The minus sign is in-
serted since we will subsequently include the effect of pump parity.
For direct coupling $(\omega_d = 0 \; , \; \Pi_p = -1)$, the normal sign convention
is restored. By expanding the derivatives and using the dynamical
equations we obtain

$$2\,\mathrm{Re}\left\{(\Pi_a \kappa_{ab}^* - \Pi_b \kappa_{ba}) \, \tilde{a}\tilde{b}d^* e^{j\beta_d z}\right\} = 0 \quad ,$$

or, for nonvanishing wave amplitudes,

$$\Pi_a \kappa_{ab} = \Pi_b \kappa_{ba}^* \quad . \qquad (39)$$

Using this result, the equations may be recast in the form

$$\left\{\frac{d}{dz} + j\beta_a\right\} \tilde{a}(z) = \Pi_a \omega_a \kappa \, d e^{-j\beta_d z} \tilde{b}*(z) \tag{40}$$

$$\left\{\frac{d}{dz} - j\beta_b\right\} \tilde{b}*(z) = \Pi_b \omega_b \kappa* \, d* \, e^{j\beta_d z} \tilde{a}(z) \quad , \tag{41}$$

where we have introduced $\kappa \equiv \Pi_a \kappa_{ab}$.

In order to solve these equations we make the change of variables

$$\hat{A}(z) = \tilde{a}(z) \, e^{j\left[\beta_a + \frac{1}{2}(\beta_d - \beta_a - \beta_b)\right]z}$$

$$\equiv \tilde{a}(z) \, e^{j\left(\beta_a + \frac{1}{2}\Delta\beta\right)z}$$

$$\hat{B}(z) = \tilde{b}(z) \, e^{j\left(\beta_b + \frac{1}{2}\Delta\beta\right)z}$$

and obtain the forms

$$\frac{d}{dz}\hat{A} = j\frac{1}{2}\Delta\beta \, \hat{A} + \omega_a \Pi_a \kappa \, d \, \hat{B}* \tag{42}$$

$$\frac{d}{dz}\hat{B}* = -j\frac{1}{2}\Delta\beta \, \hat{B}* + \omega_b \Pi_b \kappa* \, d* \, \hat{A} \quad . \tag{43}$$

After differentiating the first equation and using the second we finally obtain the result

$$\frac{d^2}{dz^2}\hat{A} - \left\{\omega_a \omega_b \Pi_a \Pi_b |\kappa d|^2 - \frac{1}{4}\Delta\beta^2\right\}\hat{A} = 0 \quad , \tag{44}$$

where ω_a and ω_b are positive. This equation admits the possibility of gaining, decaying, or beating waves depending on the sign of $\Pi_a \Pi_b$

- 26 -

and on the relative magnitude of the two terms in the bracket.

It is evident in the case in which $\Pi_a \Pi_b$ is positive that any departure from synchronism, $\beta_d = \beta_a + \beta_b$, directly degrades the gain or decay constant. By applying initial conditions and examining the energy exchanges, Tien (1958) has shown that this degradation occurs in all of the possible couplings. As in previous sections, we will use this condition as an approximation which clarifies the processes involved. Consequently, at synchronism, the solutions may be written

$$
\left\{ \begin{matrix} \hat{A}(z) \\ \\ \hat{B}(z) \end{matrix} \right\} = \left\{ \begin{matrix} \bar{A}_1 \\ \\ \bar{B}_1 \end{matrix} \right\} e^{+z|\kappa d|(\omega_a \omega_b \Pi_a \Pi_b)^{\frac{1}{2}}} + \left\{ \begin{matrix} \bar{A}_2 \\ \\ \bar{B}_2 \end{matrix} \right\} e^{-z|\kappa d|(\omega_a \omega_b \Pi_a \Pi_b)^{\frac{1}{2}}} . \qquad (45)
$$

From these forms and the power theorem (38), remembering the negative sign convention, we see

   (a) if Π_a and Π_b have the same sign (opposite small
        signal power flows), growing or decaying waves are
        possible.

   (b) if Π_a and Π_b have opposite signs (similar power
        flows), beating waves are possible.

By an argument similar to that accompanying (34) and (35), the quasi-linear power theorem (38), the perturbation solution (45) and the two preceding statements may be generalized so that they apply to both sum and difference frequency pumping. This is accomplished by the substitution $\Pi_b \rightarrow \Pi_b \Pi_p$, where Π_p is the pump parity parameter defined in (33).

The frequency and wave number relations have another use (Currie and Gould, 1960); they may be made to provide, in parametric systems, an analogy to the mode coupling diagrams of purely linear systems. This analogy results from the introduction of an _idler_ wave,

$$
\omega_b^i \equiv \omega_d - \Pi_p \omega_b \qquad (46a)
$$
$$
(\omega_d , \beta_d \text{ fixed})
$$
$$
\beta_b^i \equiv \beta_d - \Pi_p \beta_b , \qquad (46b)
$$

corresponding to the original uncoupled wave at ω_b . The use of these definitions provides a transformation of the dispersion diagram and the coupling relations as shown in Fig. 1. The model on the right in this
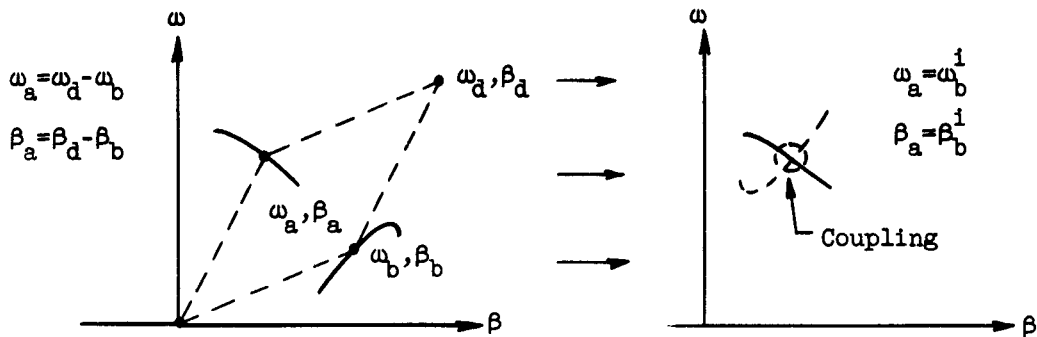
FIG. 1--Parametric idler construction.

figure conforms to that described by Pierce (1954). He showed for linear systems, as we have for quasi-linear ones, that the dynamical character of the interaction, whether a real or imaginary exponent appears in (45), depends on the power theorem (38).

A final distinction must be made in the case where the exponent is real (wave number perturbation imaginary). We must be able to tell, a priori, the difference between true amplification from which useful power may be extracted and evanescence as in a cutoff waveguide.

Empirical evidence for many diverse systems has shown that this distinction may be made solely from a knowledge of the group velocity of the uncoupled modes. Since group velocity is a kinematic property of a system, Sturrock (1958b; Polovin, 1962) conceived the idea of a purely kinematic approach to the problem. From a discussion of the types of quasi-monochromatic wave packets characterizing amplification and evanescence, Sturrock proceeds to a determination of the type of dispersion relation necessary to support these test packets. The criterion which he derives is, for a lossless system, that amplification at frequency ω_a is possible only if the coupled dispersion relation at this frequency admits both complex frequency and complex wave number. Although this

treatment applies specifically only to "direct" couplings of two propagating modes, the introduction of the concept of idler waves allows it to apply also to "displaced" or parametric coupling of the type shown in Fig. 1. The existence of these idler waves is as real physically, as the existence of spatial harmonics (Mueller, 1960). They are required by the propagating periodicity of the applied pump wave. Thus, any excitation at ω_b , β_b is accompanied by excitation at ω_b^i , β_b^i as defined in (46) and shown dotted in Fig. 1; there will also be a first order idler corresponding to ω_a , β_a which is not shown. We may now, for kinematical purposes, consider the direct interaction between the primary waves and the idler waves at the two separate points on the dispersion diagram where they cross. Since the idler transformation preserves both dynamics and group velocity, the crux of Sturrock's argument (1958b), which concerns the behavior of the dispersion relation in a vanishingly small neighborhood of any frequency of interest, will give the same result at each coupling point. Consequently, the remainder of his derivation can be carried through unchanged. Alternatively, we can consider the primary excitation at ω_a and the idler excitation at ω_a^i to be carried on two "modes" of the system and consider the various mode couplings separately as discussed in his introductory remarks.

The final results of these considerations for linear and quasi-linear systems are detailed in Fig. 2. The uncoupled modes are shown lightly dashed and the coupled modes are in bold face. The imaginary parts of the frequency and wave number are shown by the dotted curves.

It should be particularly noticed that Π_a , Π_b and Π_p the parity parameters, only appear in product. Since the slow and fast space-charge waves have similar group velocities, an examination of the beam-circuit power theorem (35) shows that a slow wave in sum frequency interaction with a circuit wave produces the same result as a fast wave in difference frequency interaction with a similar circuit wave. Since a backward circuit wave will remove positive energy excitation from a fast wave under conditions of direct coupling (difference frequency equals zero) as shown in Fig. 2b, a properly designed sum frequency coupling with a backward circuit wave should allow the similar removal of negative energy from the slow wave. This explanation of the operation of the parametric refrigeration coupler will be developed in succeeding sections.

KINEMATICAL DISTINCTIONS

	Similar uncoupled power flow $\Pi_a \Pi_b \Pi_p = -1$	Opposite uncoupled power flow $\Pi_a \Pi_b \Pi_p = +1$
Opposite uncoupled group velocities $\left.\dfrac{\partial \omega_a}{\partial \beta_a} \middle/ \dfrac{\partial \omega_b}{\partial \beta_b}\right. < 0$	a) Spontaneous oscillation	b) Evanescent transfer
Similar uncoupled group velocities $\left.\dfrac{\partial \omega_a}{\partial \beta_a} \middle/ \dfrac{\partial \omega_b}{\partial \beta_b}\right. > 0$	c) Beating waves	d) Amplification
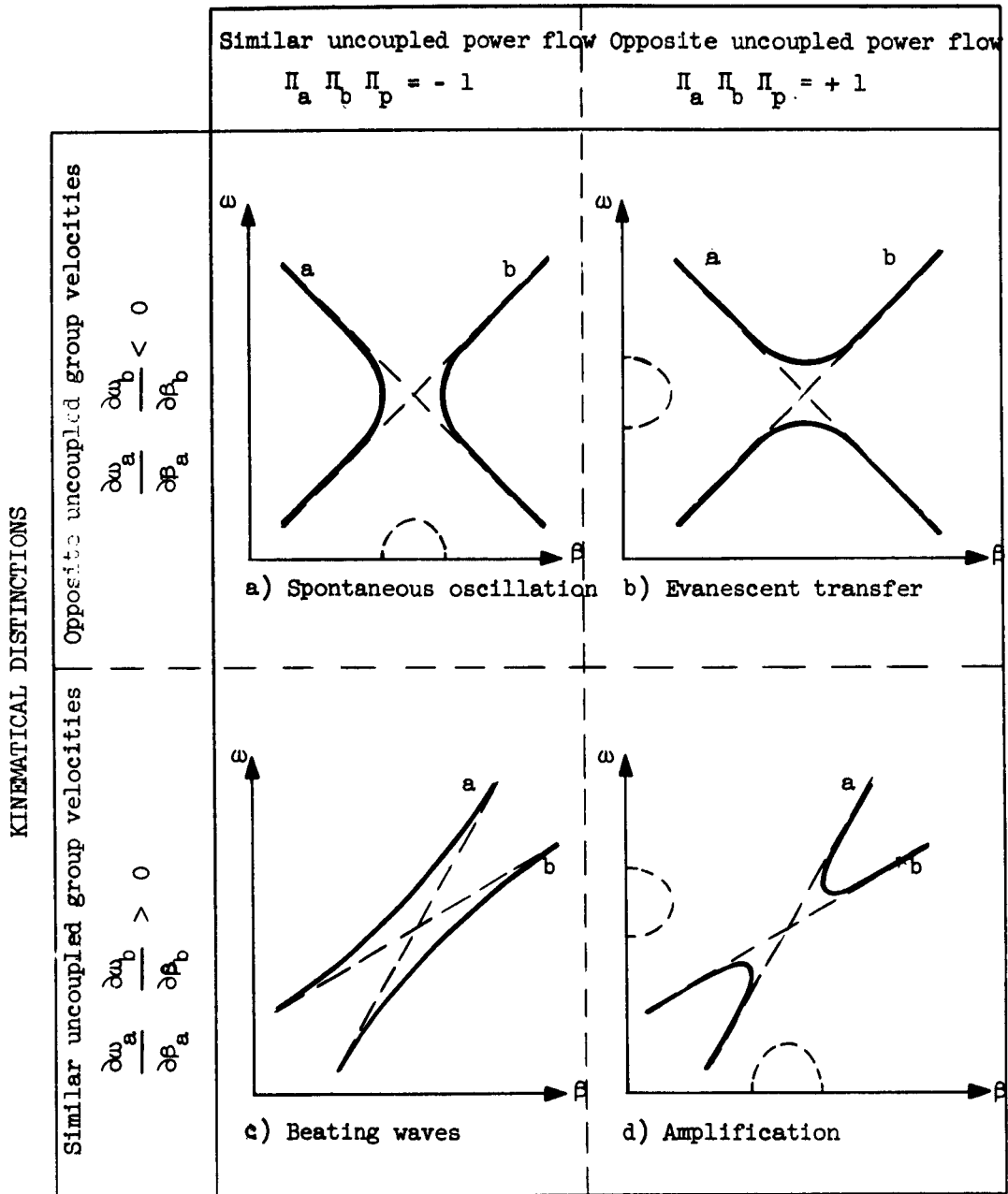
*In the absence of pumping $\Pi_p = -1$

Fig. (2)-- Interactions in a two mode system.

B. COUPLED MODE FORM OF SECOND ORDER BEAM-CIRCUIT EQUATIONS

We will now develop the dynamical equations of the system (10)→(16) in terms of the normalized mode amplitudes defined previously (31), (32). By an inversion of these equations we find

$$\widetilde{E}_{c1} = \beta_{c1} \sqrt{2K_1}\, \widetilde{b}_{c1} \tag{47}$$

$$\frac{\widetilde{v}_1}{u_0} = \frac{1}{v_0} \sqrt{\frac{Z_{01}}{2}}\, (\widetilde{a}_{1+} + \widetilde{a}_{1-}) \tag{48}$$

$$R_1 \beta_p \widetilde{z}_1 = -j \frac{1}{v_0} \sqrt{\frac{Z_{01}}{2}}\, (\widetilde{a}_{1+} - \widetilde{a}_{1-}) \quad, \tag{49}$$

where the symbol K_1 designates the circuit impedance (Pierce, 1950) and Z_{01} the space-charge impedance (Bloom and Peter, 1954) at frequency ω_1 .

The transformation of the six equations (10) → (16) using these definitions is quite direct and results in the four formal equations (50) → (53):

$$\left\{ \frac{\partial}{\partial z} + j \left(\beta_{e1} \mp R_1\beta_p\right) \right\} \widetilde{a}_{1\pm}$$

$$= -\frac{1}{2} \beta_{c1} \sqrt{\frac{K_1}{Z_{01}}}\, \widetilde{b}_{c1} - \frac{1}{4} \beta_{c2} \sqrt{\frac{K_2}{Z_{01}}}\, \widetilde{z}_d \frac{\partial}{\partial z} \widetilde{b}^*_{c2}$$

$$- j \frac{1}{4} R_2\beta_p \left(\frac{R_2^2 - R_1^2}{R_2^2}\right) \sqrt{\frac{Z_{02}}{Z_{01}}}\, \widetilde{z}_d \frac{\partial}{\partial z} (\widetilde{a}^*_{2+} - \widetilde{a}^*_{2-})$$

$$- j \frac{1}{4} R_2\beta_p \left(\frac{R_d^2 - R_1^2}{R_2^2}\right) \sqrt{\frac{Z_{02}}{Z_{01}}}\, (\widetilde{a}^*_{2+} - \widetilde{a}^*_{2-}) \frac{\partial \widetilde{z}_d}{\partial z}$$

$$- j \frac{1}{8} \frac{1}{R_2\beta_p} \sqrt{\frac{Z_{02}}{Z_{01}}}\, (\widetilde{a}^*_{2+} - \widetilde{a}^*_{2-}) \frac{\partial}{\partial z} \left(\frac{\widetilde{E}_{cd}}{v_0}\right) \quad, \tag{50}$$

and

$$\left\{ \frac{\partial}{\partial z} + j \, \beta_{c1} \right\} \tilde{b}_{c1} = \frac{1}{2} \, \Pi_{c1} \, \beta_{c1} \sqrt{\frac{K_1}{Z_{01}}} \, (\tilde{a}_{1+} - \tilde{a}_{1-})$$

$$+ \frac{1}{4} \, \Pi_{c1} \, \beta_{c1} \, \frac{\omega_1}{\omega_2} \sqrt{\frac{K_1}{Z_{02}}} \, \frac{\partial}{\partial z} \left\{ \tilde{z}_d (\tilde{a}_{2+}^* - \tilde{a}_{2-}^*) \right\} \quad , \quad (51)$$

$$\left\{ \frac{\partial}{\partial z} - j \, (\beta_{e2} \mp R_2 \beta_p) \right\} \tilde{a}_{2\pm}^*$$

$$= - \frac{1}{2} \, \beta_{c2} \sqrt{\frac{K_2}{Z_{02}}} \, \tilde{b}_{c2}^* - \frac{1}{4} \, \beta_{c1} \sqrt{\frac{K_1}{Z_{02}}} \, \tilde{z}_d^* \, \frac{\partial}{\partial z} \, \tilde{b}_{c1}$$

$$+ j \, \frac{1}{4} \, R_1 \beta_p \left(\frac{R_1^2 - R_2^2}{R_1^2} \right) \sqrt{\frac{Z_{01}}{Z_{02}}} \, \tilde{z}_d^* \, \frac{\partial}{\partial z} \, (\tilde{a}_{1+} - \tilde{a}_{1-})$$

$$+ j \, \frac{1}{4} \, R_1 \beta_p \left(\frac{R_d^2 - R_2^2}{R_1^2} \right) \sqrt{\frac{Z_{01}}{Z_{02}}} \, (\tilde{a}_{1+} - \tilde{a}_{1-}) \, \frac{\partial \tilde{z}_d^*}{\partial z}$$

$$+ j \, \frac{1}{8} \, \frac{1}{R_1 \beta_p} \sqrt{\frac{Z_{01}}{Z_{02}}} \, (\tilde{a}_{1+} - \tilde{a}_{1-}) \, \frac{\partial}{\partial z} \left(\frac{\tilde{E}_{cd}^*}{V_0} \right) , \quad (52)$$

$$\left\{ \frac{\partial}{\partial z} - j \, \beta_{c2} \right\} \tilde{b}_{c2}^* = \frac{1}{2} \, \Pi_{c2} \, \beta_{c2} \sqrt{\frac{K_2}{Z_{02}}} \, (\tilde{a}_{2+}^* - \tilde{a}_{2-}^*)$$

$$+ \frac{1}{4} \, \Pi_{c2} \, \beta_{c2} \, \frac{\omega_2}{\omega_1} \sqrt{\frac{K_2}{Z_{01}}} \, \frac{\partial}{\partial z} \left\{ \tilde{z}_d^* (\tilde{a}_{1+} - \tilde{a}_{1-}) \right\} \quad . \quad (53)$$

As an example of the derivation, (10) and (11) may be combined to give
(50) by writing

$$(50) = \frac{V_0}{\sqrt{2 \, Z_{01}}} \left[(11) \pm j \, R_1 \beta_p \, (10) \right] \quad ,$$

- 32 -

where (n) signifies the total equation (n) . The pump quantities, $\tilde{z}_d$ and $\tilde{E}_{cd}$, have been kept in their original form in order to retain full freedom in choosing the most desirable physical form for this wave in any particular application.

Once again it must be emphasized that these equations are, in a sense, symbolic in that they include all of the possible sum frequency inter-actions in an electron stream - circuit system. In any practical config-uration great care would be taken to eliminate all couplings except the one of interest. For example, in the traveling-wave amplifier there is no pumping modulation, $\beta_d = 0$. Thus, (50), (51) assume the form of (40), (41) with

$$\kappa d = -\frac{1}{2} \Pi_s \frac{\beta_c}{\omega} \sqrt{\frac{K}{Z_0}} , \qquad (54)$$

$\Pi_a = \Pi_s$, and $\Pi_b = \Pi_p \Pi_c = -\Pi_c$. The frequency subscripts, being super-fluous have been dropped. In the fast space-charge wave amplifier which we have previously discussed, no circuit is included so that all of the circuit wave terms disappear. When the remaining terms in the remaining equations (50), (52) are examined, it may be seen that they assume the form of (40), (41) with coupling constant,

$$\kappa d = \frac{1}{4} \Pi_{s1} \Pi_{s2} \beta_p \sqrt{\frac{R_1 R_2}{\omega_1 \omega_2}} \left\{ \frac{\beta_1 R_1^2 + \beta_2 R_2^2}{R_1 + R_2} \right\} \hat{z}_d , \qquad (55)$$

wherein $d \equiv \hat{z}_d$ and $\beta_d \approx \beta_1 + \beta_2$ have been used.

Another restriction, which applies to our entire analysis, is that we have only included three-frequency coupling. In particular, this restriction has produced severe practical consequences in the case of the fast space-charge wave amplifier. Although the amplifier produced the expected qualitative results (Ashkin, 1958), significant amounts of

coupling to unwanted idler frequencies,

$$\omega_{a,b}^{j} = \omega_d + \omega_{a,b}$$

$$\omega_{a,b}^{k} = 2\omega_d - \omega_{a,b}$$

$$\omega_{a,b}^{\ell} = 2\omega_d + \omega_{a,b} \quad , \tag{56}$$

$$\begin{matrix} \cdot & \cdot & \cdot \\ \cdot & \cdot & \cdot \\ \cdot & \cdot & \cdot \end{matrix}$$

effectively eliminated the noise advantage which this complicated method
of amplification was to have had (Ashkin, et al., 1959). The intrinsic
difficulty is that space-charge waves have limited dispersion and, conse-
quently, the other half of the higher idler coupling relations

$$\beta_{a,b}^{j} = \beta_d + \beta_{a,b}$$

$$\beta_{a,b}^{k} = 2\beta_d - \beta_{a,b}$$

$$\beta_{a,b}^{\ell} = 2\beta_d + \beta_{a,b} \tag{57}$$

$$\begin{matrix} \cdot & \cdot & \cdot \\ \cdot & \cdot & \cdot \end{matrix}$$

are approximately satisfied (Monson, 1960). Several attempts to mitigate
this problem (Ashkin et al., 1959; Cook, et al., 1960) have been unsuccessful.

In the experimental configuration which we will describe and verify,
(Chapter V) any modes of the system which could support higher idler
frequencies (56) will be far removed from wave number synchronism (57).
Thus, we might expect the three-frequency analysis that we have developed
to give realistic results.

C. SPECIALIZATION TO NONLINEAR COUPLING OF CIRCUIT WAVES AND STREAM WAVES

With an understanding of these restrictions, we may now discuss the important case of sum frequency coupling between space-charge waves and circuit waves. If the beam velocity is chosen so that there is no direct coupling between these waves, the equations assume the forms

$$
\left\{ \frac{\partial}{\partial z} + J \left(\beta_{el} - \Pi_{s1} R_1 \beta_p \right) \right\} \tilde{a}_1 = - \frac{1}{4} J \beta_{c2}^2 \sqrt{\frac{K_2}{Z_{01}}} \, \tilde{z}_d \, \tilde{b}_{c2}^* \qquad (58)
$$

and

$$
\left\{ \frac{\partial}{\partial z} - J \beta_{c2} \right\} \tilde{b}_{c2}^* = \frac{1}{4} J \Pi_{s1} \Pi_{c2} \frac{\omega_2}{\omega_1} \beta_{c2}^2 \sqrt{\frac{K_2}{Z_{01}}} \, \tilde{z}_d^* \, \tilde{a}_1 \qquad (59)
$$

The introduction of the space-charge parity parameter Π_{s1} allows the equations to be applied alternatively to fast or slow wave coupling, and the synchronism condition $\beta_d \approx \beta_{c2} + \beta_{el} - \Pi_{s1} R_1 \beta_p$ has been inserted. This separation is particularly useful in the case of large space-charge.

It should be noticed that these equations and the relevant power theorem (35) are once again in the quasi-linear form of (40), (41) and (38) with

$$
\kappa d = - \frac{1}{4} J \Pi_{s1} \beta_{c2}^2 \frac{1}{\omega_1} \sqrt{\frac{K_2}{Z_{01}}} \, \hat{z}_d \qquad (60)
$$

A comparison of this physical system with that detailed in Fig. 2 shows, for sum frequency pumping, the results of Table I.

TABLE I

INTERACTIONS RESULTING FROM SUM FREQUENCY COUPLING

	Slow Space-Charge Wave	Fast Space-Charge Wave
Forward Circuit Wave	Beating Waves (Parametric Kompfner Dip)	Exponential Traveling-Wave Amplification
Backward Circuit Wave	Evanescent Interchange of Excitation	Resonant Oscillation (or Amplification)

When these results are compared with those for direct (nonpumped) coupling (Gould, 1955), it is evident that the difference in dynamics (35) produced by sum frequency pumping has interchanged the role of the slow and fast space-charge waves.

With the noise problem in mind, Table I indicates two possibilities for the removal of slow wave excitation. The first would couple the slow wave to a forward wave circuit to produce a parametric Kompfner Dip (Kompfner, 1950; Hutter, 1960). Since a sensible approach to the problem suggests a helix operated in its broadband, circularly symmetric mode for the second or amplifier circuit, it would be most practical to use a helix for the noise removal coupler also. Helix spatial harmonics may be discarded as supports for the circuit and pump waves (they must both be angularly varying to strip the important angularly symmetric slow wave) by virtue of their lower coupling impedance (Harman, 1954) and generally greater complexity for use in a parametric device. This leaves the forward wave fundamental which, in a normal helix, suffers from a lack of dispersion similar to that which has plagued the fast wave amplifier. A possible way around this difficulty would be the use of a dispersive helix of the type proposed by Birdsall (1953), but the danger of problems with unwanted idlers argues against this configuration as a first choice.

For these reasons, the higher impedance fundamental spatial harmonics of a helix were chosen to support the circuit excitations. By putting the pump on the forward wave and the signal on the reverse wave (negative

group <u>and</u> phase velocity) the interaction would occur at a low voltage. The resulting (high perveance) beam would most nearly reproduce the large space-charge conditions which make the coupled mode analysis particularly valid. This configuration, and its experimental verification, will be described in the next chapter.

CHAPTER V

REVERSE WAVE PARAMETRIC INTERACTIONS

As a result of the considerations which we have developed, the
fundamental spatial harmonics of a helix were used to support parametric
coupling with the electron stream waves. In particular, the signal
excitation was to be carried by the reverse wave fundamental, ensuring
a low voltage, large space-charge, interaction. The possible inter-
actions, as predicted by the theory of Chapter IV, include the transfer
of excitation from the slow wave to the circuit and reverse wave ampli-
fication. Both of these couplings should be free of any problem with
unwanted second order interactions. Because this configuration, by design,
exhibits a near ultimate in idler dispersion, it requires a relatively
high level of pump power. A specific calculation of the predicted
effects and their experimental verification are described in this
chapter.

A. DESCRIPTION OF THE SYSTEM

The waves which may propagate on a physical system containing a
helical transmission line and a cylindrical electron stream are shown
in Fig. 3. The discrete helix, being a periodic transmission line,
propagates an infinite series of spatial harmonics (Sensiper, 1955);
only the lowest order, or fundamental, forward and backward waves are
shown here. The electron beam propagates an infinite series of space-
charge waves (Hahn, 1939; Branch and Mihran, 1955), with phase velocities
higher or lower than the electron velocity; only those with the lowest
order of radial variation and no angular variation are shown. The
separation of the two space-charge waves is, at constant current,
proportional to $u_0^{-3/2}$, where u_0 is the beam velocity. Thus, at
the relatively low beam voltages used in this device, the large space-
charge condition prevails.

$$\omega_q = \omega_{sc} + \omega_c$$
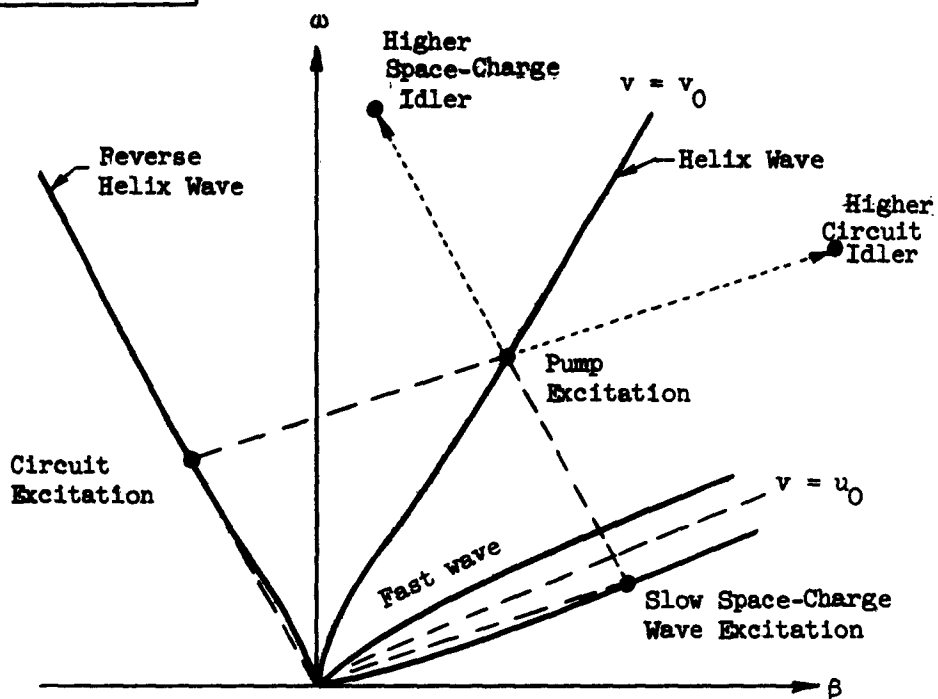
$$\beta_q = \beta_{sc} + \beta_c$$

FIG. 3-- Dispersion diagram of low voltage electron beam
enclosed in a helix showing parametric vector coupling.

Also shown in Fig. 3 are the components of the vector sum coupling relation (in the box) and one arrangement proposed to satisfy this relation. The parallelogram details the primary interaction, and the two lowest undesired idlers (56), (57) are also shown. It is evident that there are no primary uncoupled modes of the system supported at these points and, thus,.there is no possibility for an unwanted second order interaction. The lowest possible unwanted interaction is of third order; an example is that between the circuit excitation and the higher space-charge idler.

When the sum frequency circuit idler (46) is constructed, the dispersion diagram assumes the form shown in Fig. 4. The dynamical character of the interactions, predicted by the power theorem (35), with $\Pi_{cl} = -1$ and $\Pi_p = +1$, is also shown.

Finally, the behavior of the coupled modes, illustrated by the two possible independent ways of applying the boundary conditions (Appendix B), is shown in Fig. 5. The circuit power and space-charge power are defined by

$$P_{cl} \equiv \Pi_{cl} \, \tilde{b}_{cl}^{\,2} \tag{61a}$$

$$P_{s2} \equiv \Pi_{s2} \, \tilde{a}_2^{\,2} \tag{61b}$$

and the directions of signal transmission, given by the respective uncoupled group velocities, are shown by the arrows. When the fast wave coupling is increased to the point where $k\ell = \frac{\pi}{2}$, spontaneous oscillation occurs, excited by the input noise. The slow wave coupling under conditions of circuit excitation can be used to show the sense in which this is a "refrigeration" and not just a "heat exchange" interaction. Integration of the power theorem (35) with these initial conditions yields the result

$$P_{s2}(\ell) = \frac{\omega_2}{\omega_1} \left[P_{cl}(\ell) - P_{cl}(0) \right] \tag{62a}$$

$$\omega_{sc} = \omega_d - \omega_c \equiv \omega_c^p$$

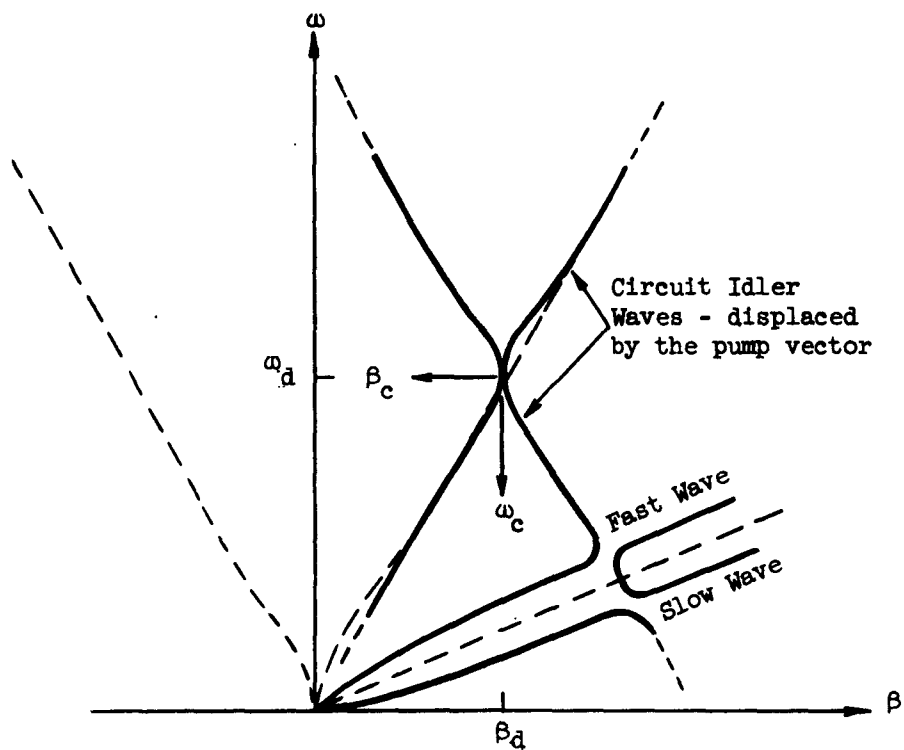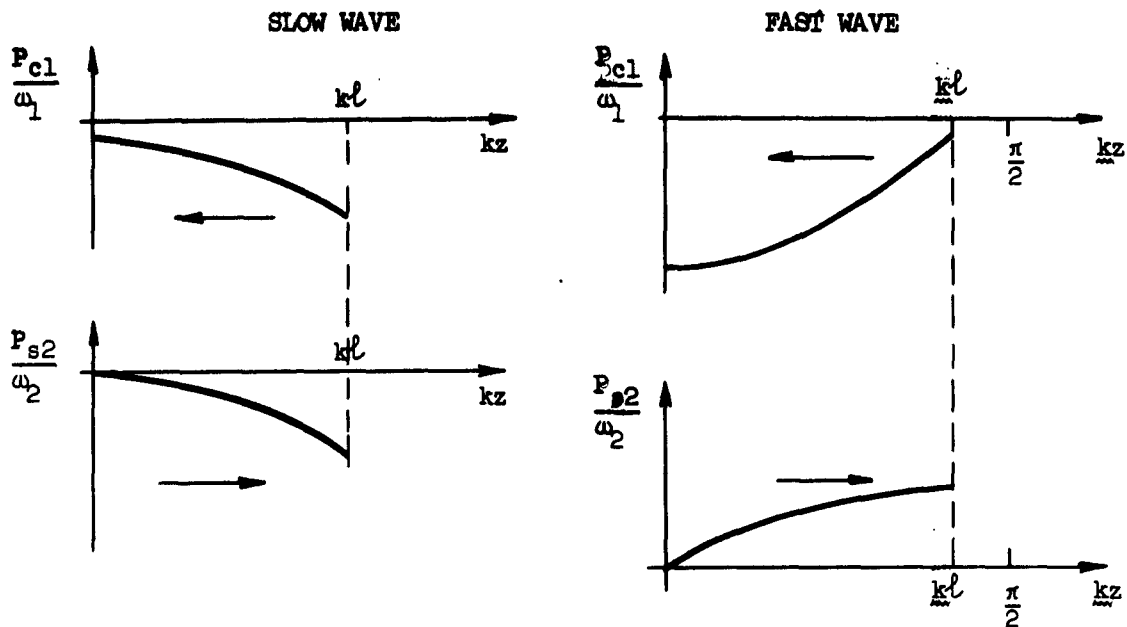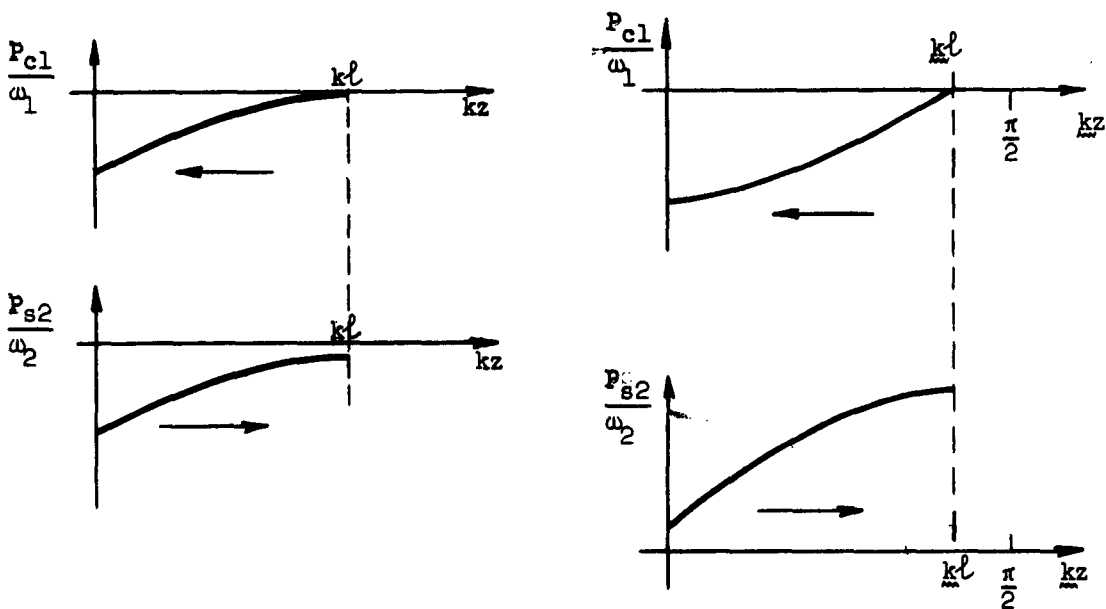$$\beta_{sc} = \beta_d - \beta_p \equiv \beta_c^p$$

FIG. 4-- Circuit idler construction showing dynamical character of space-charge wave coupling.

SLOW WAVE   FAST WAVE

a) CIRCUIT EXCITATION

b) STREAM EXCITATION

FIG. (5)-- Reverse wave circuit interactions
            with sum frequency pumping.

- 42 -

or

$$|P_{s2}(\ell)| \leq \frac{\omega_2}{\omega_1} |P_{c1}(\ell)| \qquad . \qquad (62b)$$

In a useful experimental configuration $P_{c1}(\ell)$ would be the Johnson noise output of a cooled termination, which is proportional to the temperature. Equation (62b) shows that for $\omega_2 < \omega_1$ the small-signal power leaving the coupler on the slow wave would have an even lower equivalent temperature. That is, ideally, the slow wave could be cooled to a temperature lower than those obtainable in the laboratory (Sturrock, 1959).

In order to be more specific about the amount of coupling that can be expected, we will now develop the expression for the coupling co-efficient in terms of the specific phenomenological constants of the system. The pump wave will be driven by forward circuit excitation at ω_d . From (8), we may write

$$d \equiv \hat{z}_d = \eta \, \hat{E}_{cd} \, [(\omega_d - u_0 \, \beta_{cd})^2 - R_d^2 \, \omega_p^2]^{-1}$$

$$\approx \eta \, \hat{E}_{cd} \, (\omega_d - u_0 \, \beta_{cd})^{-2} \qquad (63)$$

$$= \eta \, \beta_{cd} \, \sqrt{2K_d \, P_{cd}} \, (\omega_d - u_0 \, \beta_{cd})^{-2} \qquad ,$$

where we have neglected the space-charge force under the present conditions of synchronism wherein $\omega_d - u_0 \, \beta_{cd}$ is very large. In addition we have introduced the applied circuit pump power by using (31).

Thus, the perturbation in wave number as given by (45) and (63) becomes

$$\beta_1 \rightarrow \beta_1 + k \equiv \beta_1 \pm |\kappa d| \, \sqrt{- \, \omega_1 \omega_2 \, \Pi_{s1} \, \Pi_{c2}}$$

$$= \beta_1 \pm \frac{1}{4} \, \beta_{c2}^2 \sqrt{\Pi_{s1} \, \frac{\omega_2}{\omega_1} \, \frac{K_2}{Z_{01}}} \, \hat{z}_d$$

- 43 -

and

$$= \beta_1 \pm \frac{1}{4} \; \eta \; \frac{\beta_{c2}^2 \, \beta_{cd}}{(\omega_d - u_0 \, \beta_{cd})^2} \sqrt{\Pi_{sl} \frac{\omega_2}{R_1 \omega_p} \frac{K_2 K_d}{Z_b} P_{cd}}$$

$$\tag{64a}$$

$$= \beta_1 \pm \frac{1}{8} \; \frac{\beta_{c2}^2 \, \beta_{cd}}{(\beta_{ed} - \beta_{cd})^2} \sqrt{\Pi_{sl} \frac{\omega_2}{R_1 \omega_p} \frac{K_2 K_d}{Z_b^2} \frac{P_{cd}}{P_0}} \quad ,$$

in which $\beta_{ed} \equiv \omega_d / u_0$ is the beam wave number at ω_d , the definition of (30) has been used, and $P_0 \equiv V_0 I_0 \equiv Z_b^{-1} V_0^2$ is the dc power in the beam. All frequencies are positive, so, for slow wave coupling $(\Pi_{sl} = -1)$, the perturbation in wave number becomes an attenuation constant as predicted by the construction in **Fig. 5**.

Until now we have only considered the ideal case in which there are no resistive circuit losses. The experimental results which we will describe relate only to the "electronic" effect of parametric coupling, not to the net effect. Thus, in the calculation leading to (64a), we are able to neglect any loss in the circuit signal mode. Loss in the pump mode, d , poses a different problem. The required modification to the coupling equations is shown in Appendix B, as is the resulting change in the form of the mode solutions. Fortunately, when the over-all device is considered, the only correction is applied to the perturbed phase shift,

$$kL \; \rightarrow \; \frac{kL}{\alpha_d L} \; (1 - e^{-\alpha_d L}) \quad . \tag{64b}$$

In this expression $\alpha_d L$ is equal to the pump wave loss divided by 8.69 .

B. EXPERIMENTAL CONFIGURATION

In order to verify this analysis, an S-band (2-4 Gc) traveling-wave amplifier, modified by the removal of its attenuator, was used. The relevant measured and calculated parameters of this tube are given in Table II for some typical frequencies. For our special purposes this tube proved to have two drawbacks. The circuit loss was larger

TABLE II. CIRCUIT CHARACTERISTICS OF THE EXPERIMENTAL COUPLER

	1.3 Gc	1.4 Gc	2.7 Gc
Circuit Synchronous Voltage		560 V	395 V
Circuit Impedance, K		690 Ω	87 Ω
Circuit Loss, 8.69 αL		- 5.5 db	- 9.5 db
Ratio of Reduced Plasma Frequency to Frequency at Unit Circuit Perveance*	104		83
Active Circuit Length, L	23 cm		
Coupled Helix Length, ℓ	1.3 cm		

*This number, when multiplied by the square root of the circuit perveance, gives $R\omega_p/\omega$ (Branch, 1955).

and the focusible low voltage beam current was smaller than had been expected. These discrepancies combined to make quantitative observations difficult to achieve.

Coupled helix input and output transducers were used so that the excitation of the high wave number pump frequency space-charge modes could be minimized (See Appendix C). These couplers were approximately one space-charge wavelength long, and thus served to reduce the abruptness of the input and output boundary conditions. Finally, means were constructed and inserted whereby the diode region of the electron gun could be resonated. Thus, beam waves at frequency ω_1 could be directly excited in the vicinity of the cathode. This signal input is equivalent, at a detectable level, to the noise input under normal operating conditions.

The experimental coupler, along with the rf test circuitry, is shown in the schematic of Fig. 6 including typical values of the frequencies used. For simplicity of display, both the pump and signal generators were pulsed. The shorter pump pulse (inverted on the oscilloscope face)
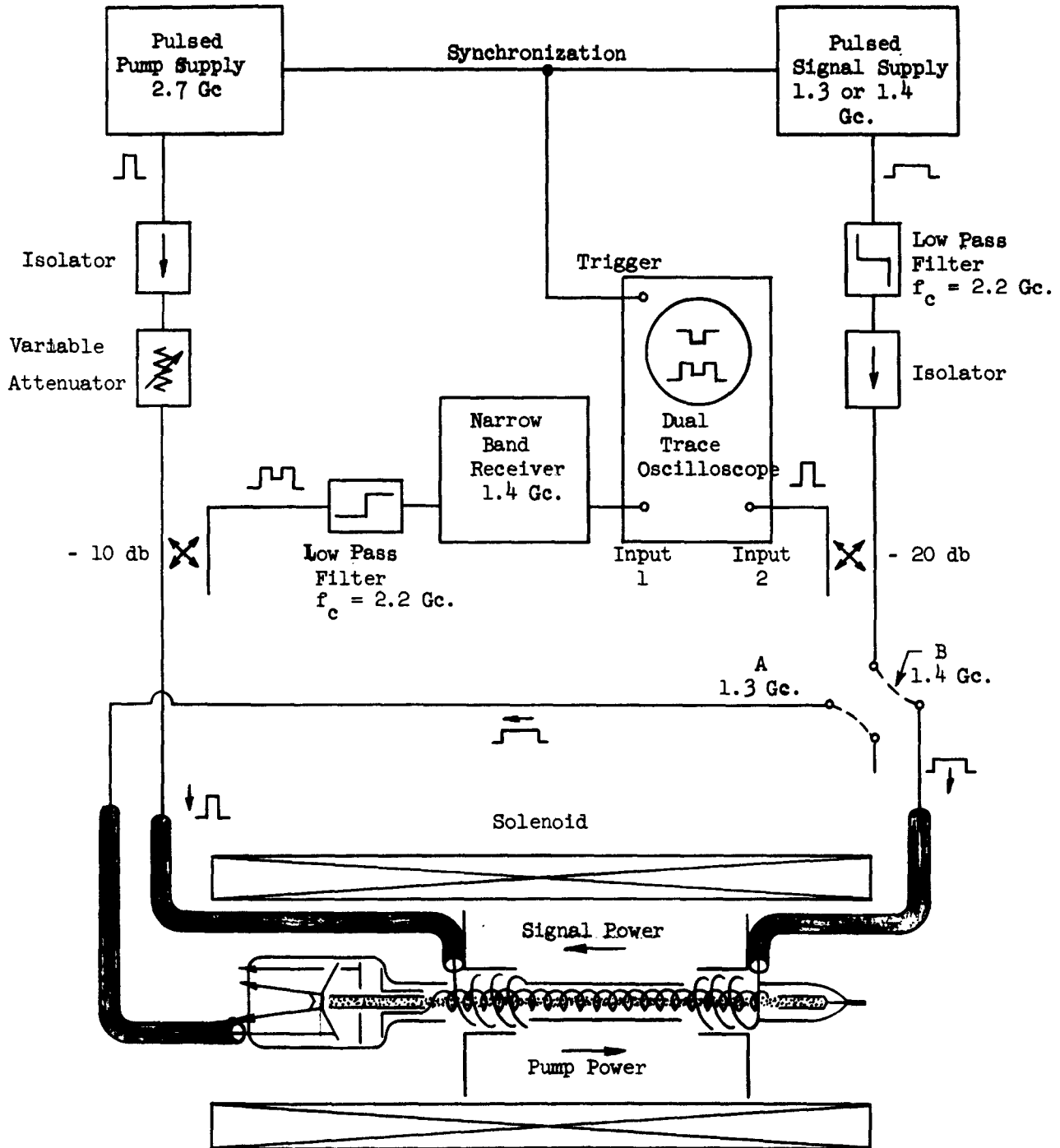
FIG. 6-- Experimental Schematic.

was synchronized in the center of the longer signal pulse. During most of the experiments the narrow band receiver consisted of a mixer (with local oscillator) and a 10 Mc bandwidth intermediate frequency amplifier. The low level, low frequency signal generator was protected against the transmitted pump power by an isolator with reverse loss greater than 35 db and a low pass filter.

The solenoid provided a strong focusing field for the electron stream at all voltages above the vicinity of limiting perveance. The voltages and currents needed to form the beam were provided by external dc power supplies which are not shown. Provision for 60 cycle modulation of the helix voltage was included.

The optimization of one of the parametric interactions required the adjustment of the beam current, helix voltage and pump power level. The observations will be discussed in the following sections.

C. INTERACTIONS VERSUS VOLTAGE

The dynamics of two-mode coupling, as given by (45) and summarized in Fig. 5, insure the symmetry of changes in the level of parametrically coupled modes. Thus, any reduction in amplitude of the circuit excitation in parametric refrigeration is proportional to the increase in amplitude of the slow wave and vice versa. The simplest verification of the presence of these interaction would, therefore, be obtained through observation of the easily accessible backward circuit wave. This method of excitation corresponds to that shown in Fig. 5a.

When the beam current and pump power were applied, the predicted interactions were observed. They are shown, displayed against beam voltage, in Fig. 7. The heavy reference line is the beam-off transmission level. As we have previously claimed, the relatively low beam voltage causes the fast wave (left hand, lower voltage) and slow wave interactions to be well separated. At slow wave synchronism the exchange of excitation with the (unmodulated) beam produces a reduction of excitation from the circuit signal during the pump pulse. The circuit frequency is 1375 Mc, the pump frequency is 2710 Mc, and the range shown is 40-65 volts at one milliampere.
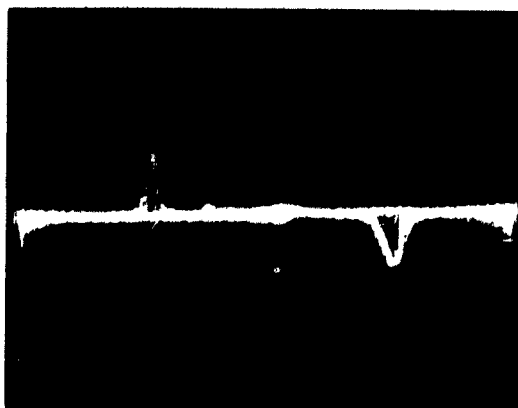
- 47 -

FIG. 7-- Reverse wave parametric interactions
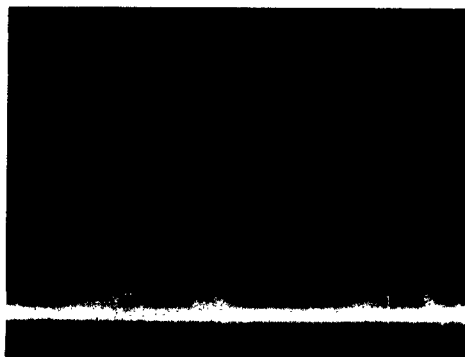displayed vs voltage.

FIG. 8-- Circuit output at 1.4 Gc
with cathode input at 1.3 Gc.

The symmetric complements of these interactions are shown in Fig. 8 at a pump level which is nearer to the oscillation threshold. In this case the slow and fast space-charge waves have been excited at the cathode by the application of a 1300 Mc signal to the beam forming electrode. With the (reverse) circuit input terminated and a 2700 Mc pump signal applied, the circuit wave output was observed with a narrow-band 1400 Mc receiver. Thus, this is a view of the circuit wave output with input conditions corresponding to those of Fig. 5b.

We first notice that the left hand or fast wave output displays the familiar resonant behavior of a backward wave amplifier near the oscillation threshold. The output on the right hand side of this figure is even more interesting. We see here a signal which has traveled from the cathode, via the "negative energy" slow space-charge wave to the vicinity of the helix and thence to the reverse circuit wave. This is a direct display of the parametric refrigeration interaction.

Figures 9 and 10 show a superposition of the two methods of observation in order to make the voltage and frequency correspondences clearer. The upper trace of each picture was made with the circuit input terminated and the gun region excited at frequency ω_1 (connection A of Fig. 6). The circuit output was detected at frequency $\omega_2 = \omega_d - \omega_1$. Then without changing any of the coupling parameters or the detection frequency, the low level signal generator was switched to the circuit input (connection B) and tuned to frequency ω_2. These traces show the symmetries predicted by Fig. 5 and, particularly, they show the removal of excitation from the slow space-charge waves.

As a final verification that these interactions are those predicted by our analysis, the circuit idler dispersion diagram of Fig. 4 was measured. In this determination, the beam current and pump power were reduced until the smallest observable interaction remained. At this point the peak and valley of Fig. 7 come together (low current, low space-charge) to form a horizontal S-curve. The voltage of the center of the S is then measured as a function of frequency. These data are plotted in Fig. 11 for two pump frequencies. The values predicted from (46) and the measured circuit dispersion diagram are shown as dotted lines, for comparison. The discrepancy at low voltage is caused by a
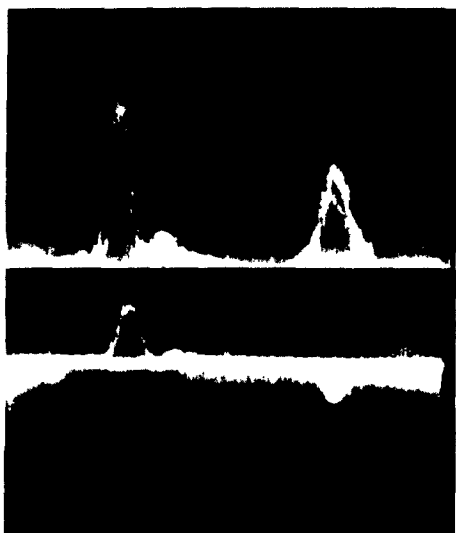
FIG. 9 -- Circuit output with
cathode excitation
at 1.3 Gc.(top) and
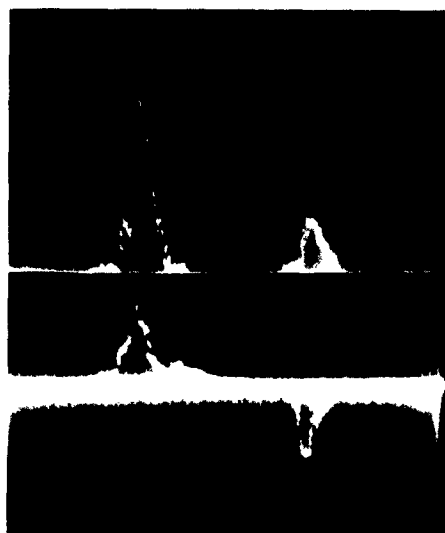with circuit excita-
tion at 1.4 Gc(bottom).

FIG. 10 --Circuit output with
cathode excitation
at 1.1 Gc. (top) and
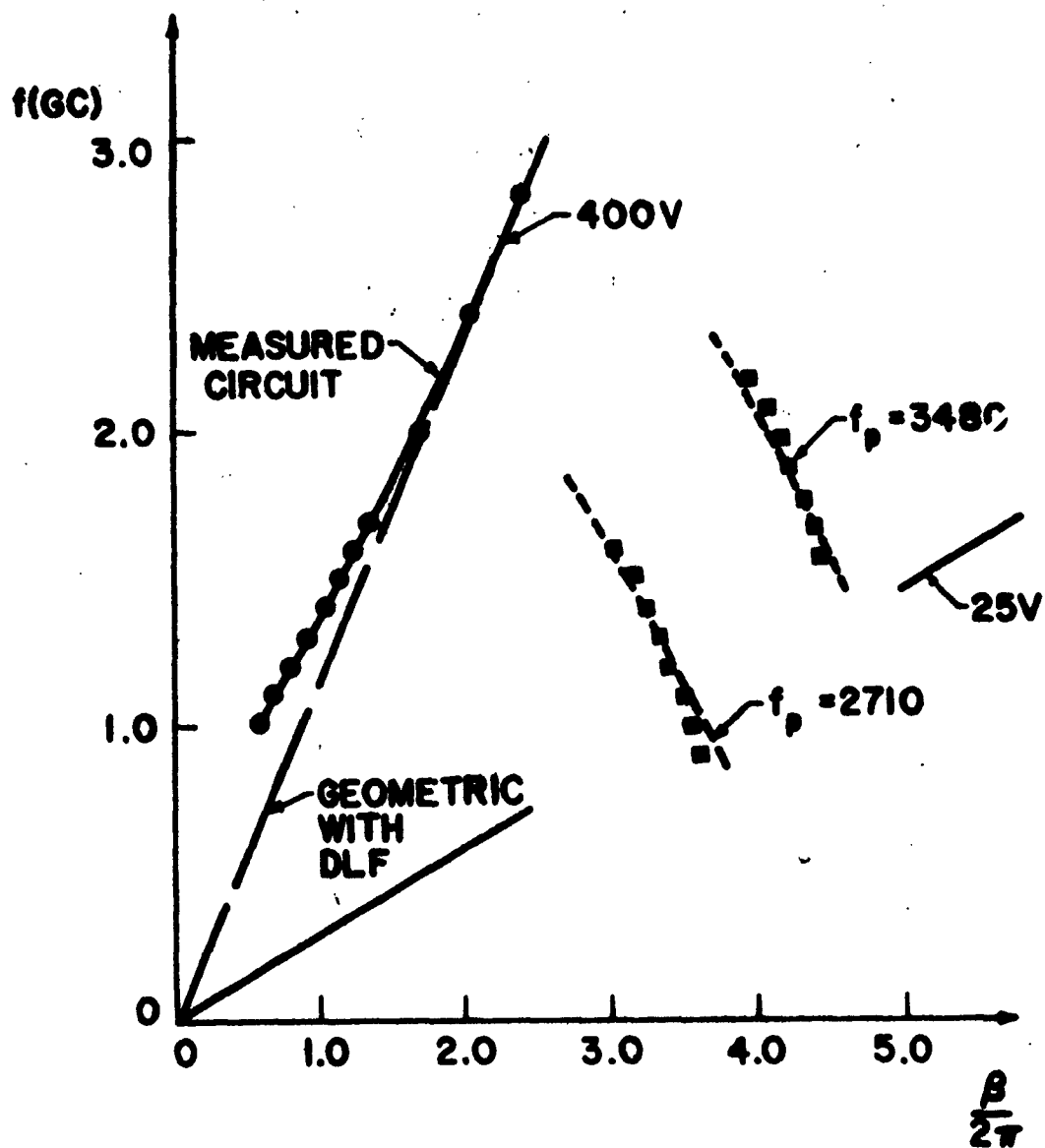with circuit excita-
tion at 1.6 Gc.(bottom).

FIG. 11--Dispersion diagram with predicted and observed parametric
interactions.

degradation in beam flow conditions at high perveance. This figure shows the value of the idler wave construction for predicting interactions.

D. REVERSE WAVE AMPLIFICATION AND OSCILLATION

With the input signal connected to the circuit and the voltage set for reverse wave amplification (See Fig. 6, connection B), the oscilloscope display assumes the form of Fig. 12. The upper trace shows the pump pulse, inverted for convenience of viewing. During the pump pulse the signal is amplified. For this picture the narrow-band heterodyne receiver was replaced by a traveling-wave amplifier so that the full 30 Mc bandwidth of the oscilloscope could be used. With this display the relation of the amount of gain to the pump amplitude is made clearer, the output following the ripples in the pump pulse.

The characteristic drawback of backward wave amplifiers may also be seen. Due to the resonant character of the gain (Fig. 5), it is very sensitive to small variations in voltage. This is shown by the haziness of the top of the gain peak.

If the current and pump power are sufficiently increased (while tracking the fast wave synchronous voltage), the considerations of the previous chapter predict the onset of spontaneous oscillation. This occurs in Fig. 5 when $k\ell = \pi/2$. This phenomenon was observed with the experimental coupler and is shown in Fig. 13. Included in the photograph is a phantom trace made by turning off the pump and turning on the signal generator. The peak power output of this signal was measurable and it is used as a calibration. The experimental conditions under which this trace was obtained are shown in Table III. Once again, Fig. 13 exhibits the familiar characteristics of a backward wave oscillation. That is, the oscillation comes on slowly (after the pump pulse) because the random input excitation must travel along the beam and then back along the circuit to the output.

E. PARAMETRIC REFRIGERATION

At a beam voltage corresponding to slow wave synchronism with the circuit idler, the output signal with circuit input assumes the form shown in Fig. 14. This photograph was taken with a traveling-wave
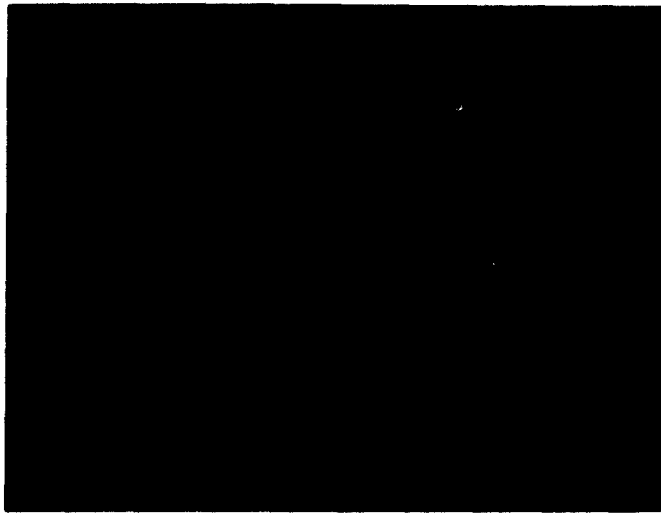
FIG. 12--Reverse wave parametric amplification.
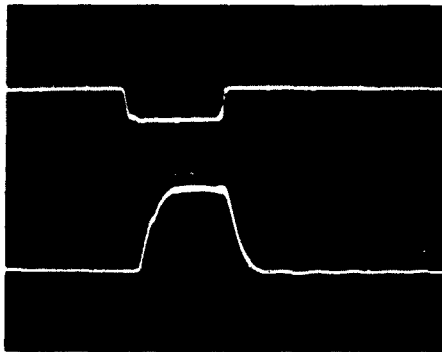
FIG. 13--Reverse wave parametric oscillation
with calibration trace.
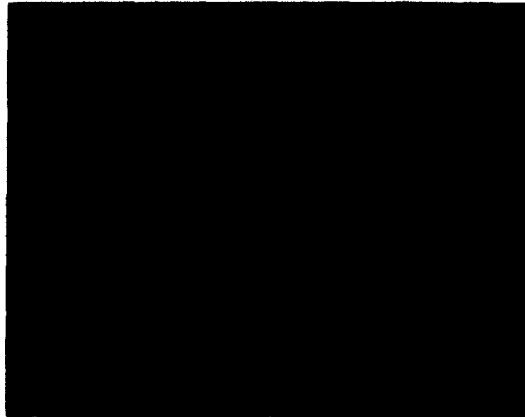
FIG. 14-- Parametric refrigeration using
reverse circuit wave.

FIG. 15-- Parametric refrigeration with
calibration trace at -5. db.

TABLE III.   EXPERIMENTAL CONDITIONS FOR REVERSE WAVE OSCILLATIONS

Signal Frequency	1435	Mc
Pump Frequency	2695	Mc
Collector Current	1020	μa
Helix Current	695	μa
Helix Voltage	40.5	volts
Peak Pump Power	380	watts
Calibration Trace	- 7	dbm

amplifier in the display circuit, as previously described, so that the pump and signal pulses both experienced the same (oscilloscope) bandpass characteristic. The relationship of the attenuation, or refrigeration, to the pump amplitude is clearly shown.

Due to the loss and perveance limitations of this coupler, which we have mentioned, quantitative results were difficult to obtain. In one experiment the display of Fig. 15 was recorded. The light calibration trace was measured in the absence of pump modulation. The experimental conditions of this photograph are shown in Table IV. With a knowledge

TABLE IV.   EXPERIMENTAL CONDITIONS FOR PARAMETRIC REFRIGERATION

Signal Frequency	1410	Mc
Pump Frequency	2695	Mc
Collector Current	390	μa
Helix Current	10	μa
Helix Voltage	50.0	volts
Peak Pump Power	180	watts
Calibration Trace	- 5	db

of the circuit wave numbers (Fig. 11), the tube parameters (Table II),
the input coupler loss (- 1.7 db), and the space-charge properties
determined by the departure from synchronous voltage ($R_1 \omega_p/\omega_1$ = .06) ,
we may use (64) to calculate the effect predicted by the theory. When
this is done the value $k\ell = j\ 1.55$ is obtained in the absence of pump
loss. When the circuit loss of 9.5 db at 2.7 Gc is taken into account
(64b), this result reduces to $k\ell = j\ 0.95$. By using the results of
Appendix B, we may make the following comparison:

Circuit Refrigeration (theory, no loss)   = - 7.8 db

Circuit Refrigeration (theory, pump loss) = - 3.4 db

Circuit Refrigeration (experiment)   ~ - 5.5 db   .

This agreement of theory with experiment is held to be reasonable. One
explanation of the discrepancy is the difficulty of estimating the space-
charge parameter, $R\omega_p$. In addition, the conditions of the analysis,
particularly that of synchronous pumping, were not exactly fulfilled.
For example, the modulation index (25) (63) varied, due to pump loss,
between the limits $0.42 < |m| < 1.24$ over the length of the circuit.
The larger value represents a fair degree of saturation which usually
produces a variation in the local beam velocity. The analytical form
(64) is quite sensitive to this parameter. The effect of a lossy
pump wave, although it degraded our observations, was not pursued fur-
ther. Any application of the principle of parametric refrigeration
would, of necessity, be designed around an extremely low loss circuit.

The major aims of our experimental program have been achieved.
We have shown the existence of nonlinear coupling to circuit modes and,
using this interaction, we have demonstrated parametric refrigeration.

CHAPTER VI

RESULTS AND RECOMMENDATIONS

Any interpretation of the results which we have obtained must relate them to the problem of low noise amplification at microwave frequencies. As we have mentioned in the Introduction, noise reduction is the only reason for using these relatively complex parametric coupling configurations.

In this chapter we will discuss the general double-stage noise problem under the assumption of single beam wave coupling. The noise performance predicted by our experimental results will be calculated as an example. In the next section the single pump wave restriction is examined. It is shown that the use of coupled helix input and output transformers effectively eliminates the deleterious excitation of pump frequency space-charge waves. The greatest practical problem, the high level of pumping modulation required, is discussed and some improvements suggested. Finally, several proposals for alternative configurations are developed with emphasis on modes of operation which will make it possible to use the wide bandwidths inherent in traveling-wave amplifiers.

A. NOISE PERFORMANCE

In discussing noise generation in devices with several stages, it is helpful to focus our attention on the noise power existing at various points in the system. One way of expressing this power is to relate it to the noise output of a resistor at a certain temperature. For example, we may describe the noise generated in a linear amplifier by referring it to the output of a matched resistor connected across the input terminals. By this usage the internally generated noise power, in a bandwidth Δf, is given by

$$N_a = kT_a \Delta f \tag{65}$$

referred to an input termination at a temperature T_a . The use of an
effective internal amplifier temperature as a measure of noise performance
has the advantage that it does not depend on any external reference. The
more commonly used noise figure required the introduction of a reference
temperature, usually taken to be that of the input circuitry. The corre-
spondence, for a single signal noise channel, is given by the relation

$$F \equiv 1 + \frac{T_a}{T_i} , \qquad (66)$$

where T_i is the input reference temperature. If the signal is subsequently
used at an intermediate frequency, care must be taken that any input noise
in the local oscillator image channel is rejected (or filtered out).
Otherwise the usable noise figure is twice this value.

In electron stream amplifiers of the traveling-wave type, we may
relate the noise temperature to the cathode temperature in a conceptually
useful way. Using a model wherein the noise in the beam is due to the
uncorrelated, fully random fluctuations of velocity and current at the
potential minimum, Haus and Robinson (1955) have developed a minimum noise
figure theorem for direct-coupled amplifiers. Their result states that
any high gain amplifier with lossless circuits has a noise temperature

$$T_a \geq (4 - \pi)^{1/2} T_c = .925 T_c , \qquad (67)$$

which is independent of space charge and of any noise reduction mechanism
in the interaction region. Thus, the limiting noise output of a linear
amplifier is determined by conditions in the gun region and, in the case
of no correlation, is approximately measured by the cathode temperature, T_c .

We will now apply the effective temperature concept to an estimation
of the noise reduction properties of the parametric refrigeration coupler.
A large space-charge traveling-wave amplifier may be described by the
direct coupling of a forward circuit wave and the slow space-charge wave.
Thus, the theory of Chapter IV applies with κ given by (54). The
analytical form of the solution, using the pertinent initial conditions,

is given in Appendix B. In addition, the transfer coefficient formalism of Haus and Robinson (1955) is introduced. This method allows the treatment of a complex device, such as a traveling-wave tube, as a "black box" or mode junction in which, for example, $|M_{ba}^{l0}|^2$ signifies the power conversion from mode a at $z = 0$ to mode b at $z = l$. In the high gain case suitable to the use of (67), consideration of the specific forms of M_{ba}^{l0} and M_{bb}^{l0} (Appendix B) shows that their ratio

$$\left| \frac{M_{bb}^{l0}}{M_{ba}^{l0}} \right| = \text{ctnh } kl$$

approaches unity. By this reasoning the result (67) can be used to estimate that the noise output of a large space-charge traveling-wave amplifier is caused by a (negative energy) slow wave noise input corresponding to a resistor at $T \sim T_c$. Since no rf power leaves the gun region except through the beam output, the Chu kinetic power theorem may be used to assert that the fast wave carries positive energy noise of an equal temperature.

Using these assumptions we may construct the simplified model of a two-stage, single-channel, parametric amplifier shown in Fig. 16.
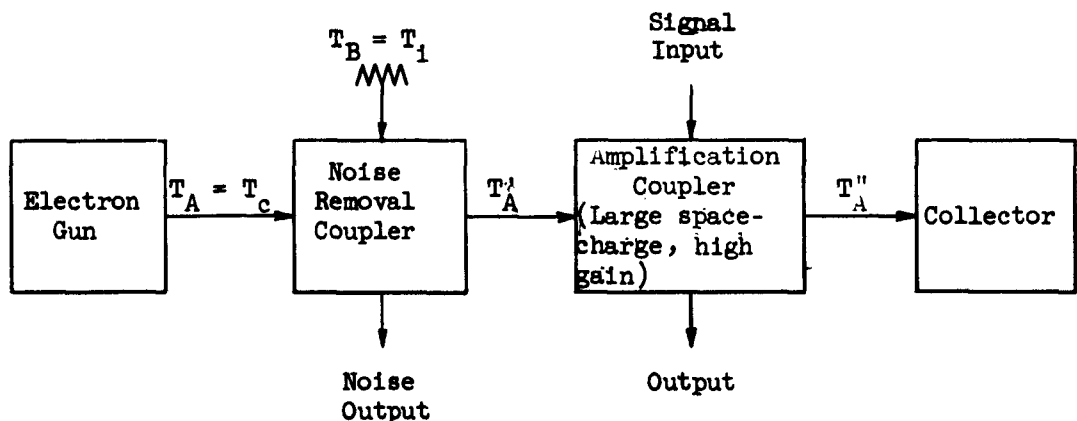
FIG. 16--Two-Stage, Two-Mode, Parametric Amplifier.

Since it is a design requirement for a practical device that any possibility
of coupling to unnecessary noise carrying modes be removed, only one beam
mode is shown. We have demonstrated, in the case of the parametric
refrigeration coupler, that this single mode coupling can be achieved.
The temperature T_i is that of the input termination of the noise removal
coupler. This and all other terminations are assumed to be perfectly
matched. The signal input is applied to the amplification coupler instead
of to the noise removal coupler since it may be shown that this always
results in a higher output signal-to-noise ratio except in the special
case that the noise removal is ideal and then it makes no difference.

With these understandings, the effective noise temperature of a high
gain, large space-charge, parametric amplifier is given by

$$T_a = T_A' = \left| M_{ab}^{O1} \right|^2 T_1 + \left| M_{aa}^{O1} \right|^2 T_c \ ,$$

where, for example, M_{ab}^{O1} is the power transfer coefficient from circuit
mode B at its input to beam mode A at its output. These transfer
coefficients are defined and calculated in Appendix B. This form for
the noise temperature shows the necessity, in a two-stage device, for
cooling the input termination, T_i .

As an illustration of this method of calculation we will apply it to
the parametric refrigeration coupler of Chapter V, (Section A). By using
the results of Appendix B, we may obtain

$$T_a = T_A' = \left| M_{ab}^{\ell\ell} \right|^2 T_1 + \left| M_{aa}^{\ell o} \right|^2 T_c$$

$$= T_1 \frac{\omega_a}{\omega_b} \tanh^2 k\ell + T_c \operatorname{sech}^2 k\ell \ ; \tag{68}$$

the analytical value of k is given by (60). For an ideal coupler,
$k\ell \to \infty$, the beam is truly "refrigerated" for $\omega_a < \omega_b$.

If we now use the experimental values of Tables II and IV with

$$\text{sech}^2 \, k\ell \sim - \, 5.5 \quad \text{db}$$
$$T_1 \sim \quad 290^\circ \, K$$
$$T_c \sim \quad 1020^\circ \, K \quad ,$$

we may calculate the value

$$T_a \sim \frac{1.385}{1.410} \, (1 - 0.28) \, (290) + (0.28) \, (.020) \; = \; 490^\circ \, K$$

for the effective temperature of the output slow beam wave. If this beam were now introduced into a low-voltage, high-gain, traveling-wave amplifier circuit, a noise figure

$$F \; = \; 4.3 \, \text{db}$$

(referred to room temperature) would be predicted.

It is evident, from the derivation of this result, that much of the output noise is produced in the input termination. The application of a cooling bath, for example, liquid nitrogen at $77^\circ \, K$, to both circuit and termination would greatly improve this result. Since this step would effectively eliminate the deleterious effects of pump loss, the amount of refrigeration would approach more nearly the theoretical low loss value

$$\text{sech}^2 \, k\ell \sim - \, 7.8 \, \text{db} \quad .$$

Using these data, a recalculation predicts

$$T_a \sim 230^\circ \, K$$

for the noise content of the output slow wave. Upon the application of this large space-charge beam to a traveling-wave amplifier circuit, a single channel noise figure

$$F \sim 2.5 \text{ db}$$

at 1.4 Gc would be obtained.

The second major approach in the attempt to get around the strictures of the minimum noise figure theorem involves the introduction of forced correlation into the gun region. Through the use of long, low voltage, drift regions, values of the correlation parameter

$$\alpha_c \equiv \frac{T_a}{T_c}$$

as low as 0.25 have been obtained at S-band (Currie and Forster, 1959). Since this mechanism is applied to a separate physical region of the amplifier it is basically different from the parametric process that we have discussed and may, in fact, be used in concert with it. This addition, at frequencies near 2 Gc , would result in effective noise temperatures of the order of 60°K.

It must be emphasized that these results are predictions derived from a particular experimental configuration. However, the fact that the most serious of the unwanted idler couplings can be eliminated by the general method of parametric beam-circuit coupling gives hope that results like these are possible.

The greatest practical problem standing in the way of such useful applications of dispersive parametric coupling is discussed in the next section.

B. PUMP WAVE CONSIDERATIONS

The provision of large idler dispersion and, consequently, the inhibition of unwanted interactions depends on the ability to support a pump wave which is removed (in phase velocity) from the beam waves. This

may be accomplished by using a circuit wave to carry the pump excitation, as we have done, but this configuration raises two serious problems.

On the one hand, it must be realized that the electron beam is the only nonlinear element of the system. Thus, the useful pump modulation is that given by (63). It is evident, from the denominator of this expression and from our experimental results, that any increase of the pump-to-beam wave number separation above the minimum required to produce idler dispersion has a large adverse effect on the pumping efficiency.

One possibility for the mitigation of this difficulty is the use of a properly dispersive circuit. For example, a helix with a transversely conducting shield exhibits greatly enhanced positive dispersion (Birdsall, 1953; Kino, 1953). An application of the vector coupling diagram for reverse wave interactions (Fig. 3) shows that a dispersion increase in this direction always reduces the denominator of (63). In addition, Kino (1953) has shown that this improvement is accompanied by a substantial increase in the beam coupling impedance. For very dispersive circuits this increase can approach two orders of magnitude and can, thereby, lead to a substantial increase in pump efficiency. Although this discussion has dealt, for definiteness, with the reverse wave coupler, similar improvements in pump wave impedance are possible in other configurations through the use of coupled helix circuits (Cook, Kompfner, and Quate, 1956).

This conception leads to a solution of the second practical difficulty connected with the pump wave. The requirement of a pump wave removed in phase velocity from the beam waves means that care must be taken that the space-charge normal modes at the pump frequency are not excited. If they were excited at substantial levels the spurious idler difficulties endemic to fast space-charge wave amplifiers would again appear.

The problem of unwanted stream wave excitation is entirely analogous to the problem of mode conversion caused by discontinuities in a multi-mode waveguide. In an axially uniform stream-circuit system with an electron velocity far removed from synchronism, no interaction is possible and the circuit and space-charge modes are orthogonal to each other as are the modes of a waveguide.

If the circuit is approximately uniform throughout its length, the largest contribution to spurious space-charge mode excitation is due to

imperfections in the transformers between the input/output transmission lines and the circuit. A treatment of this effect is developed in Appendix C and, in particular, the use of coupled helix transducers is evaluated. The theory shows that the amplitudes of the various beam waves are related to the spatial Fourier transform of the circuit pump amplitude appearing at the beam. In particular, the amplitude of the beam wave at wave number β_1 is proportional to the Fourier transform evaluated at $k = \beta_1$.

The results for the coupled helix are given because they are characteristic and, what is more important, this type of transformer is an eminently practical solution to the problem. If the coupled helix has a length ℓ , which results in complete excitation transfer to the helix (Cook, et al., 1956), the unwanted space-charge wave modulation depth (25) is related to the forced circuit wave modulation depth as (see Appendix C)

$$\left| \frac{m_{s,f}}{m_c} \right| = \left| \frac{\hat{z}_{s,f}}{\hat{z}_c} \right| \sim \frac{\pi}{4R_d \beta_p \ell} \quad , \tag{69}$$

where s and f refer to to the slow and fast space-charge waves.

This order of magnitude result holds under the coupler circuit and describes the relative strength of the most important spurious parametric interactions. One restrictive condition is central to the analysis and to the simplicity of this form, namely

$$(\beta_{ed} - \beta_{cd}) \, \ell \gg \frac{\pi}{2} \quad ,$$

which means that the beam is far from synchronism.

A similar problem in the parametric refrigeration configuration is that of the residual pump excitation which leaves the noise removal coupler. This modulation may severely restrict the operation of the following direct coupled amplifier section (Forster, 1960). Beyond the circuit $m_c \equiv 0$ but $m_{s,f}$ are, as we show in Appendix C, relatively unchanged. Thus, (69) may also be used to give the magnitudes of the unwanted space-charge excitations incident on the amplifier section, relative to the necessary circuit wave excitation in the coupler.

With this understanding (69) shows that two prominent pumping wave problems, those of spurious space-charge interactions (Ashkin, Cook, and Louisell, 1959) and of unwanted modulation in the amplifier section (Forster, 1960), may be effectively eliminated by the use of coupled circuit transducers of sufficient length.

The latter of the problems discussed in this section relates only to the configuration in which a parametric noise removal coupler is followed by a direct-coupled amplifier. We will now treat several proposed variants of this type and of its reverse, in which the noise removal section is direct coupled.

C. ALTERNATIVE CONFIGURATIONS

The reverse wave parametric coupler which we have verified experimentally and discussed as an example has certain drawbacks. Since it depends on a backward wave interaction, its instantaneous bandwidth is quite narrow and electrical or pump frequency tuning must be applied to change the frequency of operation. One possibility would be to maintain constant voltage and to tune the refrigeration interaction by means of the pump frequency. In this case the amplifier circuit could be a large space-charge (low voltage) helix operating in the fundamental mode. In order to provide an output bandwidth of one octave (second helix), the input helix must have substantial impedance, negligible dispersion, and matched input/output over about three octaves. This effect is shown, slightly exaggerated, in Fig. 17. It is felt that this approach could be useful for half-octave operation but pump frequency tuning at moderate power levels still presents practical difficulties.

In some applications the eventual signal usage is at a lower, so-called intermediate, frequency. In these cases there is an advantage in having a tunable input amplifier which rejects the intermediate frequency image noise. This noise, originating in the input circuits, travels directly through a wide band amplifier and is superimposed on the wanted signal by the action of the intermediate frequency input mixer. Thus, even with an ideal amplifier, the output signal-to-noise ratio is twice that at the input and the over-all noise figure cannot be less than 3 db.

- 65 -
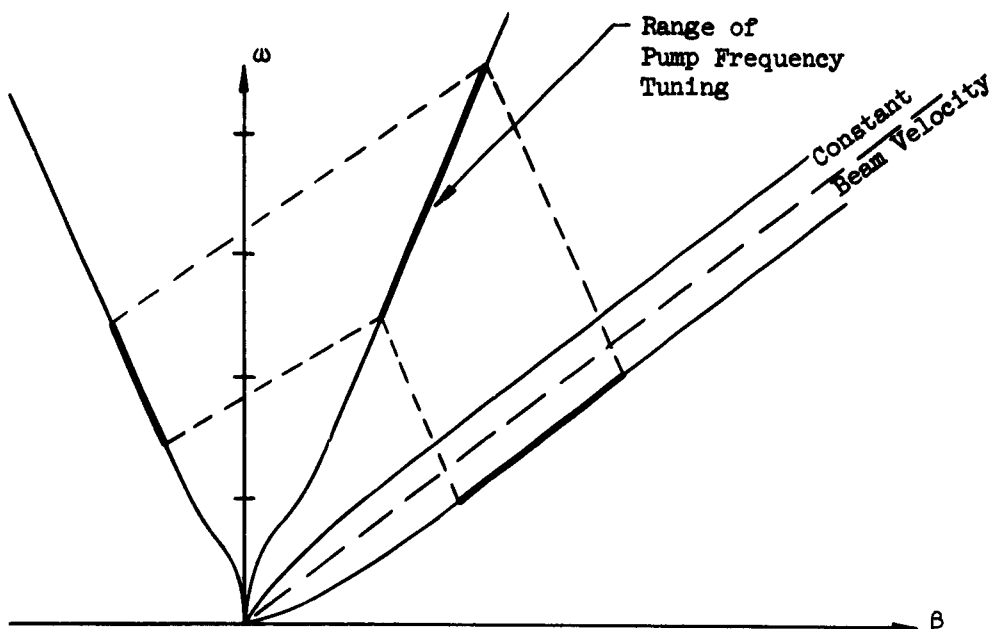
FIG. 17-- Coupling relations for octave parametric refrigeration at constant voltage.

FIG. 18-- Interdigital structure and measured dispersion diagram (Wada, 1956).

- 66 -

Since the parametric refrigeration coupler that we have treated is voltage tunable at constant pump frequency, we need only find a fundamental backward wave circuit to use in the amplifier section. The most attractive possibility appears to be a cylindrical interdigital structure (Wada, 1956) whose configuration and dispersion diagram is shown in Fig. 18. This circuit has a higher backward wave impedance in its fundamental $(n = 0)$ mode than the bifilar helix has in its commonly used $n = -1$ mode. Other possibilities are the folded waveguide circuit (Putz, et al., 1952; Hutter, 1960) or properly loaded cylindrical ladders (White, et al., 1963). If the backward wave dispersion of any of these circuits (especially the TEM-like interdigital structure which propagates at zero frequency) is made to match the circuit idler dispersion of Fig. 4, a synchronously tunable refrigerator-amplifier would be produced. Thus, high gain, narrow-band operation, with its specialized advantages, would be possible.

For other applications a configuration which requires no tuning and is more compatible with the wide bandwidths characteristic of conventional traveling-wave amplifiers is needed. One very attractive possibility involves the use of a positively dispersive helix (Birdsall, 1953; Kino, 1953) in its fundamental forward wave spatial harmonic. These helices, enclosed in a transversely conducting shield which could be approximated by a closely wound insulated helix, have already been mentioned for their relatively large coupling impedance. Their dispersion makes them additionally interesting; a typical form of forward wave parametric interaction is shown in Fig. 19.

FIG. 19--Wideband parametric interaction with a helix enclosed in a transversely conducting shield. Helix dispersion from Kino (1953).

This coupling, the parametric analog of the Kompfner dip, would produce (under large space-charge conditions) a beating wave exchange of excitation between the slow wave and the circuit wave. The resonant character of this interaction would require a careful tailoring of circuit dispersion and impedance to pr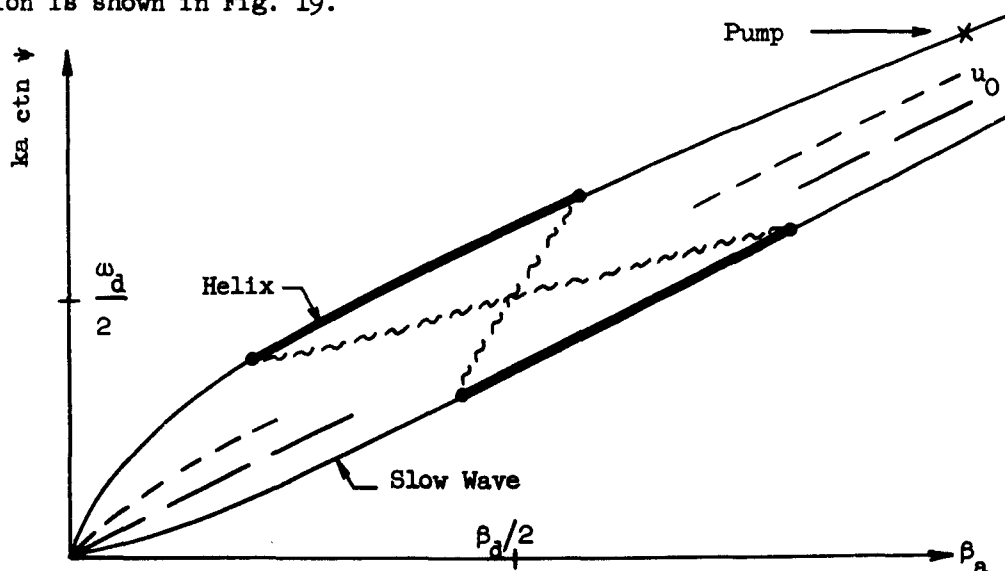oduce any appreciable bandwidth (Cook, 1955; Louisell, 1955). Nonetheless, circuit pumped parametric interactions of this general class have one great advantage; due to the relatively small velocity separation between the forward wave circuit and the beam they provide greatly improved efficiency of pump usage. As we have discussed in the section on pump waves, there is a practical upper limit to pumping efficiency set by the requirements of spurious idler dispersion. This configuration would allow that limit to be approached. It should also be mentioned that a backward wave fundamental circuit can be used for forward wave interaction. This requires the pump to be carried by the reverse wave fundamental as is shown, by way of example, in Fig. 18.

There is one remaining significant class of variants of the refrigerator-amplifier devices that we have described. They are related to these as parametric reverse wave amplification is related to parametric refrigeration. This class includes all of the circuit coupled generalizations of the original fast wave amplifier of Louisell and Quate (1958). If, in each configuration that we have proposed, the parametric and linear coupler are transposed and fast wave substituted for slow wave, a dual series of low noise amplifiers is obtained. This duality results, it is clear, from the appearance of the product $\Pi_p \Pi_s$ in the power theorem (35).

As an example of this class consider the analog of the synchronously tunable backward wave refrigerator-amplifier we have discussed. If a large space-charge beam at a current below the oscillation threshold interacts, by direct coupling, with a fundamental backward wave mode, an evanescent interchange of fast wave and (cool) circuit excitation results. If this beam is then introduced into a parametric coupler under conditions proper for reverse wave amplification, the device becomes a heat exchanger-parametric amplifier.

This result, which is essentially that predicted for the original fast space-charge wave amplifier, becomes practical through the introduction of nonlinear circuit coupling. The possibility of idler dispersion

control offered by this new degree of freedom effectively eliminates the spurious interaction problems which have made the fast wave amplifier unrealizable.

The verification of this new type of circuit coupling and the demonstration of negative energy excitation removal are the central results of this work. The application of these principles has made possible the development of a manifold of new parametric amplifier types.

CHAPTER VII

CONCLUSIONS

In the course of this paper we have developed a conception, composed of theory and experiment, of the nonlinear operation of a class of electronic wave propagating systems.

We have derived the second order physical equations, and the resulting power theorem, which describe all direct coupled and parametric interactions possible in a longitudinal electron stream-slow waveguide system. In particular, the theory predicts a new effect, nonlinear coupling of space-charge and circuit waves. This issue, conceived by Sturrock (1960c), allows a more versatile use of the parametric vector coupling relations and may be made immune to unwanted second order idler interactions. With this simplification, and the assumption of large space charge, a two-mode, quasi-linear coupling theory is developed. The existence of idler spatial-temporal harmonics is described, and they are used to create a parametrically coupled dispersion diagram. Finally, kinematical considerations are cited to produce a general criterion for predicting the result of an arbitrary parametric coupling.

An experimental coupler, a modified helix traveling-wave amplifier, which would test these predictions has been described. Nonlinear circuit wave coupling has been observed and the bases of the two-mode theory, the idler construction and large space-charge assumption, have been empirically justified. Parametric reverse wave amplification has been demonstrated, the first observation of fast space-charge wave gain without spurious second order idler interactions. At higher pump and current levels, spontaneous reverse wave oscillation occurred. Finally, the parametric refrigeration interaction has been demonstrated. It must be admitted that the experimental verification of the removal of negative energy noise is only an indirect one since the output slow wave has not been used in an amplifier. The burden of this paper, however, in which the preponderance of the theory has been directly verified, allows no

other interpretation. The experimental results have been related to the problem of low noise amplification; with the available coupling level, which is not optimal, and external circuit cooling, a noise figure near 2.5 db is predicted for 1.5 Gc . Since this mechanism is fundamentally different from those used in the gun region, the addition of correlation enhancement could further lower this figure. The most important obstacles to the procurement of results such as these have been discussed. The ability, and necessity, to provide sufficient idler dispersion requires a high pump power level. A number of suggestions have been made to minimize this effect. The use of coupled helix transducers has been presented as a practical solution to the problem of unwanted pump waves. Several alternative configurations, using positively dispersive helices and circuits with a fundamental backward wave, have been proposed in an effort to provide increased bandwidth and pumping efficiency. A class of fast wave amplifiers, using parametric circuit coupling, has been described.

This report has presented a unified theoretical and experimental exposition of a new type of nonlinear electron stream-slow waveguide interaction. The versatility of this type of coupling, with respect to the control of idler dispersion, coupled with the excellent high frequency properties of space-charge waves, should allow the construction of amplifiers, in the centimeter range, with noise temperatures less than 100° K .

APPENDIX A

SPACE-CHARGE REDUCTION IN MULTIPLY-EXCITED ELECTRON
STREAMS – THE LAGRANGE EXPANSION

This appendix contains a simplified derivation of the form of the space-charge field. Starting from the results for free propagation, the effect of a second impressed wave is evaluated. The reduction factor for driven waves is shown to be a function of their wave number.

In a thin electron stream in confined flow, corresponding to the model discussed in Chapter II, the space-charge reduction factor may be introduced by a phenomenological variant of Poisson's equation,

$$\frac{\partial}{\partial z} \tilde{E}_{s1} (z_0, t) \equiv R_1^2 (\beta_1) \frac{\tilde{\rho}_1 (z_0, t)}{\epsilon_0} = \frac{R_1^2 (\beta_1)}{\epsilon_0} \hat{\rho}_1 e^{j(\omega_1 t - \beta_1 z_0)} , \quad \text{(A.1)}$$

valid for single frequency propagating excitation. The functional dependence of R_1 on β_1 is related to the space-charge dispersion equation $\omega = f(\beta)$ and is determined by the (geometric) boundary conditions (Branch and Mihran, 1955).

For slow waves $(\omega/\beta \ll c)$ the space-charge field may be adequately described as the gradient of a quasi-static potential (Pierce, 1950) and we may, in turn, find this potential by using the Green's function for the particular geometry (Sturrock, 1960a). Thus, by dropping the time dependence, the single frequency field is given by

$$\tilde{E}_{s1} (z_0) = - \frac{\partial}{\partial z_0} \int_{-\infty}^{\infty} G(z_0 - \xi_0) \tilde{\rho}_1(\xi_0) \, d\xi_0 = -\hat{\rho}_1 \frac{\partial}{\partial z_0} \int_{-\infty}^{\infty} G(z_0 - \xi_0) e^{-j\beta_1 \xi_0} d\xi_0$$

$$= j\beta_1 \tilde{\rho}_1 (z_0) \int_{-\infty}^{\infty} G(\eta) e^{-j\beta_1 \eta} \, d\eta , \quad \text{(A.2)}$$

where the last equality is achieved by a change of dummy variable and the insertion of the specific form of $\tilde{\rho}_1 (z_0)$ from (A.1). The last integral may be recognized as the Fourier transform of $G(\eta)$,

$$g(k) = \frac{1}{2\pi} \int_{-\infty}^{\infty} G(\eta) \, e^{-jk\eta} \, d\eta \quad , \tag{A.3}$$

evaluated at $k = \beta_1$. Differentiation of (A.2) reproduces the form of (A.1) and we obtain the result

$$R_1^2 (\beta_1) \equiv 2\pi e_0 \, \beta_1^2 \, g(\beta_1) \tag{A.4}$$

for the single-frequency, single-wave number, reduction factor.

In principle, the Green's function for a cylindrical charge column in any circuit environment may be calculated. The quasi-static contribution to the space-charge dispersion relation may then be derived from the Fourier transform of this result. A practical approximation, for the case of a helix, may be made by the replacement of the helix by an equivalent conducting pipe (Branch, 1955). In this case the Green's function is well known (Tien, Walker, and Wolontis, 1955).

We will now develop an expression, similar to that of (A.2), which applies to multiple frequency excitation of an electron stream. This may be achieved by the development of $\tilde{\rho}_1 (z_0)$ in a generalization of the Lagrange or inverse Taylor expansion (E. L. Chu, 1960 b; Sturrock, 1960 d). Under conditions of small amplitude excitation the total charge density at an interior beam point $z_0 + \tilde{z}$ may be expressed in a Taylor series,

$$\rho_T (z_0 + \tilde{z}) = \left\{ 1 + \tilde{z} \, \frac{\partial}{\partial z_0} + \frac{1}{2} \tilde{z}^2 \, \frac{\partial^2}{\partial z_0^2} + \ldots \right\} \rho_T (z_0) \quad . \tag{A.5}$$

In addition, the constraint of charge conservation requires

$$\rho_0(z_0)\, dz_0 = \rho_T(z_0 + \tilde{z})\, d(z_0 + \tilde{z}) = \rho_T(z_0 + \tilde{z})\left(1 + \frac{\partial \tilde{z}}{\partial z_0}\right) dz_0 \quad , \quad (A.6)$$

where the last equality comes from the introduction of the one-dimensional, infinitesimal Jacobian (Bobroff, 1959). By inverting these equations we obtain a generalization of the Lagrange expansion which relates the perturbed charge density at z_0 to the quiescent or dc charge density. This result takes the form

$$\rho_T(z_0) = \left\{ 1 + \tilde{z}\,\frac{\partial}{\partial z_0} + \frac{1}{2}\tilde{z}^2\,\frac{\partial^2}{\partial z_0^2} + \ldots \right\}^{-1} \left[\rho_0(\tilde{z}_0)\left(1 + \frac{\partial \tilde{z}}{\partial z_0}\right)^{-1} \right]$$

$$= \rho_0(z_0) - \frac{\partial}{\partial z_0}(\rho_0 \tilde{z}) + \frac{1}{2}\frac{\partial^2}{\partial z_0^2}(\rho_0 \tilde{z}^2) + \ldots \quad , \quad (A.7)$$

where the binomial expansion has been used in the last equality. [For completeness we will mention that a similar expansion for $J_T(z_0)$ may be obtained through the use of the definition

$$J_T(z_0 + \tilde{z}) = \rho_T(z_0 + \tilde{z})\, v_T(z_0 + \tilde{z}) \quad ,$$

the expression (1) for the velocity,

$$v_T(z_0 + \tilde{z}) = u_0 + \left(\frac{\partial}{\partial t} + u_0 \frac{\partial}{\partial z_0}\right)\tilde{z} \quad , \quad (A.8)$$

and (A.5) and (A.6). The resulting expression,

$$J_T(z_0) = \rho_0 u_0 + \rho_0 \frac{\partial}{\partial t}\left(\tilde{z} - \tilde{z}\frac{\partial \tilde{z}}{\partial z_0} + \ldots\right) \quad , \quad (A.9)$$

is that given by Sturrock (1960 d) and used in the circuit equation (9) of Chapter II.]

- 74 -

When (A.7) is frequency-analyzed through the use of (4) and the ω_1 component is inserted in (A.2), we obtain the result

$$\tilde{\mathbb{E}}_{s1}(z_0) = \rho_0 \frac{\partial}{\partial z_0} \int_{-\infty}^{\infty} G(z_0 - \xi_0) \frac{\partial}{\partial \xi_0} \left\{ \tilde{z}_1(\xi_0) - \frac{1}{2} \frac{\partial}{\partial \xi_0} [\tilde{z}_2^*(\xi_0) \tilde{z}_d(\xi_0)] \right\} d\xi_0$$

$$\approx \rho_0 \frac{\partial}{\partial z_0} \left[\begin{array}{c} -j\beta_1 \hat{z}_1 \, e^{-j\beta_1 z_0} \int_{-\infty}^{\infty} G(\eta) \, e^{-j\beta_1 \eta} \, d\eta \\[4mm] + \frac{1}{2} (\beta_d - \beta_2)^2 \hat{z}_2^* \hat{z}_d \, e^{-j(\beta_d - \beta_2) z_0} \int_{-\infty}^{\infty} G(\eta) \, e^{-j(\beta_d - \beta_2)\eta} \, d\eta \end{array} \right]$$

$$= -2\pi\rho_0 \left[\begin{array}{c} \beta_1^2 \, g(\beta_1) \, \tilde{z}_1(z_0) \\[4mm] - \frac{1}{2} (\beta_d - \beta_2)^2 \, g(\beta_d - \beta_2) \frac{\partial}{\partial z_0} [\tilde{z}_2(z_0) \, \tilde{z}_d^*(z_0)] \end{array} \right] \quad , \quad (A.10)$$

where the approximate equality indicates that any possible parametric space-charge wave interaction (perturbation of wave number) is small in the sense detailed by (18).

By using the result of (A.4) and the definition of the dc plasma frequency, we may now write an approximate form for the space-charge field,

$$\eta \tilde{\mathbb{E}}_{s1}(z_0) = \omega_p^2 \left\{ R_1^2(\beta_1) \tilde{z}_1(z_0) - R_1^2(\beta_d - \beta_2) \frac{1}{2} \frac{\partial}{\partial z_0} [\tilde{z}_2^*(z_0) \tilde{z}_d(z_0)] \right\} , \quad (A.11)$$

under conditions of two-frequency excitation. This form and that of (A.5) show the wave number dependence, at a given frequency, of the space-charge reduction factor. If, now, the assumption of pump wave synchronism

$$\beta_d = \beta_1 + \beta_2$$

is made, the result of (5) is obtained.

- 75 -

APPENDIX B

APPLICATION OF BOUNDARY CONDITIONS TO THE TWO-MODE COUPLER--TRANSFER COEFFICIENTS AND THE EFFECT OF LOSS IN THE PUMP WAVE

In this appendix we will develop the solutions of the quasi-linear coupling equations (42), (43) by applying the necessary initial conditions. We will also evaluate the effect of loss in the pumping wave, d .

For simplicity let us consider the case of synchronous coupling $(\Delta\beta = 0)$, in which the solutions (45) may be written

$$\hat{A}(z) = A_1 e^{kz} + A_2 e^{-kz} \tag{B.1}$$

$$\hat{B}*(z) = B_1^* e^{kz} + B_2^* e^{-kz} \quad , \tag{B.2}$$

where

$$k \equiv + |\kappa d| (\omega_a \omega_b \Pi_a \Pi_b)^{1/2} \tag{B.3}$$

has been introduced. Use of the dynamical equations (42), (43) allows the elimination of two of the arbitrary coefficients and we may then obtain

$$\hat{B}*(z) = \frac{k}{\Pi_a \omega_a \kappa d} (A_1 e^{kz} - A_2 e^{-kz}) \quad , \tag{B.4}$$

wherein A_1 and A_2 are complex constants.

The placement of boundary or initial conditions is determined by the small-signal energy velocity. We will place these initial conditions outside the region of the interaction so that the energy velocity is

unequivocally equal to the group velocity. With the understanding that mode A is a beam wave (which always has positive group velocity), there are two cases of interest.

In the first case we consider that mode B is a backward wave and its initial value is specified at the output $z = \ell$. Thus, the arbitrary constants are determined from

$$A_0 \equiv \hat{A}(0) = A_1 + A_2 \tag{B.5}$$

$$B_\ell^* \equiv \hat{B}^*(\ell) = \frac{k}{\Pi_a \omega_a \kappa d} (A_1 e^{k\ell} - A_2 e^{-k\ell}) \ . \tag{B.6}$$

These equations may be inverted and the results may be inserted into (B.1, B.2) to provide

$$\hat{A}(z) = A_0 \frac{\cosh k(\ell - z)}{\cosh k\ell} + \frac{\Pi_a \omega_a \kappa d}{k} B_\ell^* \frac{\sinh kz}{\cosh k\ell} \tag{B.7}$$

$$\hat{B}^*(z) = -\frac{k}{\Pi_a \omega_a \kappa d} A_0 \frac{\sinh k(\ell - z)}{\cosh k\ell} + B_\ell^* \frac{\cosh kz}{\cosh k\ell}$$

$$= -\frac{\Pi_b \omega_b \kappa^* d^*}{k} A_0 \frac{\sinh k(\ell - z)}{\cosh k\ell} + B_\ell^* \frac{\cosh kz}{\cosh k\ell} \tag{B.8}$$

where the definition of k has been used in the last step. It should be noted that such symmetry as there is in these equations has its root in the power theorem (38).

These equations may be recast in a form which describes the coupler as a whole as a "black box" or mode junction. This is accomplished by the introduction of transfer coefficients similar to those of Haus and

Robinson (1955). In this notation, special cases of (B.7) and (B.8) become

$$\hat{A}(\ell) = \hat{A}(0) \operatorname{sech} k\ell + \hat{B}*(\ell) \frac{\Pi_a \omega_a \kappa d}{k} \tanh k\ell$$

$$\equiv M_{aa}^{\ell 0} \hat{A}(0) + M_{ab}^{\ell \ell} \hat{B}*(\ell) \tag{B.9}$$

and

$$\hat{B}*(0) = - \hat{A}(0) \frac{\Pi_b \omega_b \kappa* d*}{k} \tanh k\ell + \hat{B}*(\ell) \operatorname{sech} k\ell$$

$$\equiv M_{ba}^{00} \hat{A}(0) + M_{bb}^{0\ell} \hat{B}*(\ell) \quad . \tag{B.10}$$

Thus, if all external terminals are matched,

$$\left| M_{ba}^{00} M_{ba}^{00*} \right| = \frac{\omega_b}{\omega_a} \left| \tanh^2 k\ell \right| \tag{B.11}$$

is the power gain or loss from mode $A(\omega_a)$ to mode $B(\omega_b)$ at the $z = 0$ terminals.

If $\Pi_a \Pi_b = -1$, all of the preceding formulae remain correct; the substitutions

$$k \to ik$$

$$\sinh kz \to i \sin kz$$

$$\cosh kz \to \cos kz \tag{B.12}$$

will make them more useful, however.

In the second case mode B is a forward wave and both initial conditions are set at $z = 0$. This may be treated as a specialization of our previous result (B.7) and (B.8) by making the identification $\ell = 0$. For variety we will treat the case $\Pi_a \Pi_b = -1$ in which k is purely imaginary. Thus we may write

$$\hat{A}(z) = A_0 \cos k\, z + \frac{\Pi_a \omega_a \kappa d}{k} B_0^* \sin k\, z \qquad (B.13)$$

$$\hat{B}^*(z) = \frac{\Pi_b \omega_b \kappa^* d^*}{k} A_0 \sin k\, z + B_0^* \cos k\, z \qquad (B.14)$$

to describe the mode amplitudes inside the coupler.

By applying these equations at the output terminals $(z = \ell)$ we may again introduce the transfer coefficients,

$$\hat{A}(\ell) = \hat{A}(0) \cos k\, \ell + \hat{B}^*(0) \frac{\Pi_a \omega_a \kappa d}{k} \sin k\, \ell$$

$$\equiv M_{aa}^{\ell 0} \hat{A}(0) + M_{ab}^{\ell 0} \hat{B}^*(0) \qquad (B.15)$$

$$\hat{B}^*(\ell) = \hat{A}(0) \frac{\Pi_b \omega_b \kappa^* d^*}{k} \sin k\, \ell + \hat{B}^*(0) \cos k\ell$$

$$\equiv M_{ba}^{\ell 0} \hat{A}(0) + M_{bb}^{\ell 0} \hat{B}^*(0) \ . \qquad (B.16)$$

When, for example, $k\ell = \pi/2$ and $\omega_a = \omega_b$, these equations describe the large QC Kompfner dip coupler in which all incident circuit excitation is transferred to the fast beam wave and vice versa.

The analyses of Chapter IV and of this appendix have concentrated on the ideal situation in which there is no resistive loss. Circuit attenuation at the signal frequency may be easily accounted for by the

substitution

$$\beta_b \rightarrow \beta_b - i\alpha_b^{'}$$

in all of the equations. Loss in the coupling, or pump, wave d enters
in a more subtle way. The synchronous mode equations (42), (43) must
then be written

$$\frac{d}{dz} \hat{A} = \omega_a \Pi_a \kappa d e^{-\alpha_d z} \hat{B}^* \qquad (B.17)$$

$$\frac{d}{dz} \hat{B}^* = \omega_b \Pi_b \kappa^* d^* e^{-\alpha_d z} \hat{A} , \qquad (B.18)$$

where α_d is the attenuation constant at the pump frequency. The solutions
to these equations have the form

$$\begin{Bmatrix} \hat{A} \\ \hat{B}^* \end{Bmatrix} = \begin{Bmatrix} \bar{A} \\ \bar{B}^* \end{Bmatrix} e^{\pm \frac{k}{\alpha_d} \left(1 - e^{-\alpha_d z} \right)} , \qquad (B.19)$$

which reduces to (B.1), (B.2) as $\alpha_d \rightarrow 0$. From this result we see that
all of our previous solutions and, in particular, the transfer coefficients,
can be corrected for pump loss by the substitution

$$k\ell \rightarrow \frac{k\ell}{\alpha_d \ell} \left(1 - e^{-\alpha_d \ell} \right) . \qquad (B.20)$$

This formula is the basis for the modification of (64b).

APPENDIX C

CIRCUIT-DRIVEN PUMP WAVES

In order to determine the distribution of pump frequency excitation among the several normal modes of a stream-circuit system we must solve the coupled differential equations (10) and (11), under the constraint of suitable boundary conditions. With the insertion of pump frequency notation, these equations may be rewritten as

$$\left(\frac{\partial}{\partial z} + j\,\beta_{ed}\right)\tilde{z}_d = \frac{\tilde{v}_d}{u_0} \tag{C.1}$$

$$\left(\frac{\partial}{\partial z} + j\,\beta_{ed}\right)\frac{\tilde{v}_d}{u_0} = -R_d^2\,\beta_p^2\,\tilde{z}_d - \frac{1}{2}\frac{\tilde{E}_{cd}}{V_0} \;, \tag{C.2}$$

where the influence of pump harmonics has been ignored.

It is well known that these equations, in the absence of the circuit driving term, may be put in a form which is characteristic of transmission line behavior (Bloom and Peter, 1954; Hutter, 1960). If $\tilde{E}_{cd}$ is introduced as a distributed series EMF , the transmission line equations may still be solved (Schelkunoff, 1943).

We will apply this method directly to the solution of the electronic equations (C.1) and (C.2), with the assumption of loose pump coupling to the beam. This assumption is physically attractive since, under the conditions of interest, the beam velocity is only a fraction $(\sim 1/3)$ of the circuit interaction velocity. With this understanding we may write

$$\tilde{E}_{cd} = \hat{E}_{cd}(z)\,e^{-j\beta_{cd}z}$$

and use for $\hat{E}_{cd}(z)$ the externally applied pump amplitude as it is seen by the beam.

By direct substitution we may verify that the forced (particular) solutions of (C.1) and (C.2) may be written in the forms

$$\frac{\tilde{v}(z)}{u_0} = -\frac{1}{4V_0} \int_0^z \tilde{E}_c(\xi) \left\{ e^{-j\beta_{sd}(z-\xi)} + e^{-j\beta_{fd}(z-\xi)} \right\} d\xi \quad (C.3)$$

$$\tilde{z}(z) = -\frac{J}{4R_d \beta_p V_0} \int_0^z \tilde{E}_c(\xi) \left\{ e^{-j\beta_{sd}(z-\xi)} - e^{-j\beta_{fd}(z-\xi)} \right\} d\xi \quad , \quad (C.4)$$

in which the undriven (homogeneous) solution wave numbers,

$$\beta_{\substack{s_d \\ f^d}} \equiv \beta_{ed} \pm R_d \beta_p \quad ,$$

corresponding to the slow/fast space-charge waves (7) have been introduced. Since we are interested in the depth of modulation (25) which depends on $\tilde{z}(z)$, we will concentrate on (C.4) which may be expanded as shown in (C.5):

$$\tilde{z}(z) = -\frac{J}{4R_d \beta_p V_0} \left\{ \begin{array}{l} e^{-j\beta_{sd}z} \int_0^z \hat{E}_c(\xi) \, e^{j(\beta_{sd} - \beta_{cd})\xi} \, d\xi \\ \\ - e^{-j\beta_{fd}z} \int_0^z \hat{E}_c(\xi) \, e^{j(\beta_{fd} - \beta_{cd})\xi} \, d\xi \end{array} \right\} . \quad (C.5)$$

We will now apply this equation, related to the Fourier transform, to the physical model for $\hat{E}_{cd}(z)$ at the beam shown in Fig. (C.1).
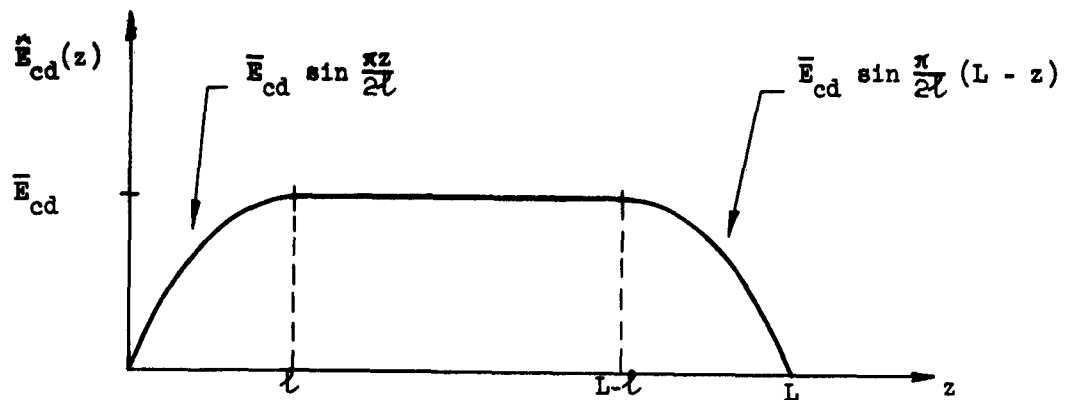
FIG. C.1--Pump field amplitude distribution on a lossless helix with coupled helix input and output transducers.

This amplitude vs distance distribution corresponds to that on a lossless helix of length L with properly designed coupled helix transformers of length ℓ (Cook, Kompfner and Quate, 1956).

The computation of the amplitudes of the various components of $\tilde{z}(z)$ is long but simple and only the results will be given. The formulas will be written in terms of a normalized phase shift,

$$ b_1 \equiv \frac{2}{\pi} \beta_{1d} \ell \ , $$

the length of the coupler region in half radians. In this notation, the

result for $\ell < z < L - \ell$ may be written

$$\tilde{z}_d(z) \left[2 \frac{\overline{E}_{cd}}{v_0} \frac{\ell^2}{\pi^2} \right]^{-1} = e^{-j\beta_{cd}z} \left[\frac{1}{(b_e - b_c)^2 - R_d^2 b_p^2} \right]$$

$$- e^{-j\beta_{sd}z} \left[\frac{j(b_s - b_c) - e^{+j(b_s - b_c)\frac{\pi}{2}}}{2R_d b_p(b_s - b_c)[1 - (b_s - b_c)^2]} \right]$$

$$+ e^{-j\beta_{fd}z} \left[\frac{j(b_f - b_c) - e^{+j(b_f - b_c)\frac{\pi}{2}}}{2R_d b_p(b_f - b_c)[1 - (b_f - b_c)^2]} \right] \quad . \quad (C.6)$$

It may be noticed that the β_{cd} excitation amplitude is completely independent of ℓ and is, in fact, that given in (8).

Two interesting special cases of this result may be given. The first, for $\ell > 0$, corresponds to the physical situation of our experiments. For example, the most unfavorable experimental conditions (in this particular respect) that we used are those described by Table IV, with. $\ell \cong 1.3$ cm, from which the values

$$b_e \cong 32$$

$$b_c \cong 11 \qquad\qquad\qquad (C.7)$$

$$R_d b_p \cong 1.6$$

may be derived. These values are characteristic and they satisfy the relations

$$b_e \;\; , \;\; b_c \gg 1$$

$$\qquad\qquad\qquad (C.8)$$

$$b_e \;\; , \;\; b_c \gg b_p \quad .$$

- 84 -

By using these approximations in (C.6) we obtain

$$\tilde{z}_d(z) \approx \frac{\overline{E}_{cd}}{2V_0} \frac{1}{(\beta_{ed} - \beta_{cd})^2} \left[e^{-j\beta_{cd}z} + \frac{j}{2R_d b_p} \left(1 - \frac{2R_d b_p}{b_e - b_c} \right) e^{-j\beta_{sd}z} - \frac{j}{2R_d b_p} \left(1 + \frac{2R_d b_p}{b_e - b_c} \right) e^{-j\beta_{fd}z} \right] , \quad (C.9)$$

and, by the insertion of (C.7), we obtain the numerical value

$$\tilde{z}_d(z) \sim \frac{\overline{E}_{cd}}{2V_0} \frac{1}{(\beta_{ed} - \beta_{cd})^2} \left[e^{-j\beta_{cd}z} + j\ 0.265\ e^{-j\beta_{sd}z} - j\ 0.360\ e^{-j\beta_{fd}z} \right] \quad (C.10)$$

for the amplitudes of the pumping waves in the parametric refrigeration experiment of Fig. 15. These results are felt to be short of the dangerous limit, but only barely so. The coupler was designed to be used at higher currents, and since the space-charge amplitudes vary roughly as the inverse square root of the current, the values were then more favorable.

The second special situation to which (C.6) applies is that in which the pump modulation is abruptly applied. In this case $\ell \rightarrow 0$ and we have

$$\tilde{z}_d(z) \approx \frac{\overline{E}_{cd}}{2V_0} \frac{1}{(\beta_{ed} - \beta_{cd})^2} \left[e^{-j\beta_{cd}z} + \frac{1}{2} \left(\frac{b_e - b_c}{R_d b_p} - 1 \right) e^{-j\beta_{sd}z} - \frac{1}{2} \left(\frac{b_e - b_c}{R_d b_p} + 1 \right) e^{-j\beta_{fd}z} \right] . \quad (C.11)$$

- 85 -

By inserting the numerical values of (C.7) we may obtain

$$
\tilde{z}_d(z) \sim \frac{\overline{E}_{cd}}{2V_0} \frac{1}{(\beta_{ed} - \beta_{cd})^2}
\begin{bmatrix}
e^{-j\beta_{cd}z} + 6.1\, e^{-j\beta_{sd}z} \\[2em]
- 7.1\, e^{-j\beta_{fd}z}
\end{bmatrix}
\quad , \qquad (C.12)
$$

indicating that abrupt circuit pump excitation would have prematurely saturated the beam and, thereby, would have completely obliterated the desired circuit pumped interaction.

One remaining application of the general result (C.5) will be given. This will relate to the question of the amount of pump modulation in the output beam of the parametric refrigeration coupler. The problems raised by the existence of residual modulation have been treated by Forster (1960). We will show that the use of an "adiabatic" transducer of the coupled helix type can effectively eliminate this problem.

The beam output modulation may be obtained from the general result (C.5) by applying it to the form of $\hat{E}_{cd}(z)$, given in Fig. C.1, in the realm of values $z > L$. As before, for $\ell > 0$, the conditions (C.8) give a meaningful approximation. With their use we find the result

$$
\tilde{z}_d(z) \cong \frac{\overline{E}_{cd}}{2V_0} \frac{1}{(\beta_{ed} - \beta_{cd})^2} \frac{j}{2R_d\, b_p}
$$

$$
\times
\begin{bmatrix}
e^{-j\beta_{sd}z}\left(1 - \dfrac{2R_d\, b_p}{b_e - b_c}\right)\left(1 + e^{j(\beta_s - \beta_c)L}\right) \\[2em]
- e^{-j\beta_{fd}z}\left(1 + \dfrac{2R_d\, b_p}{b_e - b_c}\right)\left(1 + e^{j(\beta_f - \beta_c)L}\right)
\end{bmatrix}
\qquad (C.13)
$$

for the output pump modulation. Since there is no more circuit support, the β_{cd} excitation is not allowed and has disappeared. The slow and fast waves have the same relative amplitude factor, the inverse of the length of the transition region in space-charge quarter wavelengths, that they did for $z < L - \ell$ (C.9). Now, however, there is an interference effect from the two ends of the pump circuit. Under very special circumstances, namely that

$$(\beta_{ed} - \beta_{cd})L = (m + n + 1)\pi :$$

and

$$R_d \, \beta_p \, L = (m - n)\pi$$

simultaneously, the pump output vanishes. However, since most coupler circuits are hundreds of beam wavelengths long, these conditions are impractical of attainment in that they would require unrealizable beam voltage control.

At the worst (C.13) indicates a doubling of the pump space-charge wave amplitude relative to that existing under the circuit. Thus, by using coupled helix input and output transformers which provide a sufficiently large value of $R_d \beta_p \ell$, the residual pump modulation may be made arbitrarily small.

LIST OF REFERENCES

Adler, R., Hrbek, G., and Wade, G. (1959). "The Quadrupole Amplifier, A Low Noise Parametric Device," Proc. IRE 47, 1713-1723.

Ashkin, A. (1958). "Parametric Amplification of Space-Charge Waves," J. Appl. Phys. 29, 1646-1651.

Ashkin, A., Cook, J. S., and Louisell, W. H. (1959). "Modification of the Space-Charge Wave Dispersion for Parametric Amplification," Presented at the IRE Conference on Electron Tube Research, Mexico City, Mexico, June 1959 (unpublished).

Bers, A., and Penfield, P. (1962). "Conservation Principles for Plasmas and Relativistic Electron Beams," IRE Trans. on Electron Devices ED-9, 12-26.

Birdsall, C. K. (1953). "A Simple Method for Obtaining Phase Velocity, Attenuation, and Impedance of a Sheath Helix in Arbitrary Surroundings," Report No. ETL-12, Electron Tube Laboratory, Hughes Research and Development Laboratories, Culver City, California.

Bloom, S., and Peter, R. W. (1954). "Transmission Line Analogue of a Modulated Electron Beam," RCA Review 15, 95-112.

Bobroff, D. L. (1959). "Independent Space Variables for Small Signal Electron Beam Analyses," IRE Trans. on Electron Devices ED-6, 68-78.

Bobroff, D. L. (1960). "The Coupling of Modes Theory of Longitudinal Wave Electron Beam Parametric Amplifiers," Report No. T-255, Research Division, Raytheon Mfg. Co., Waltham, Massachusetts.

Bobroff, D. L., and Haus, H. A. (1958). "Uniqueness and Orthogonality of Small Signal Solutions in Electron Beams," Report No. 31, Research Division, Raytheon Mfg. Co., Waltham, Massachusetts.

Branch, G. M., and Mihran, T. G. (1955). "Plasma Frequency Reduction Factors in Electron Beams," IRE Trans. on Electron Devices ED-2, 3-12.

Branch, G. M. (1955). "Reduction of Plasma Frequency in Electron
Beams by Helices and Drift Tubes," Proc. IRE 43, 1018.

Brillouin, L. (1946). Wave Propagation in Periodic Structures, McGraw-
Hill Book Co., New York.

Butcher, P. N. (1957). "The Circuit Equation for Traveling Wave Tubes,"
Report No. 402-1, Electron Devices Laboratory, Stanford University,
California.

Chu, E. L. (1960a). "The Lagrangian and the Energy-Momentum Tensor in
the Perturbation Theory of Classical Electrodynamics," Ann. Phys.
9, 76-92.

Chu, E. L. (1960b). "On the Concept of Fictitious Surface Charges of
an Electron Beam," J. Appl. Phys. 31, 381-388.

Chu, L. J. (1951). "A Kinetic Power Theorem," Presented at the IRE
Conference on Electron Tube Research, Durham, N. H., June 1951
(unpublished). Partial presentation in Haus and Robinson (1955).

Cook, J. S. (1955). "Tapered Velocity Couplers," Bell System Tech. J.
34, 807-822.

Cook, J. S., Louisell, W. H., and Quate, C. F. (1960). "Space-Charge
Wave Parametric Amplifiers," J. Electr. and Contr. VIII, 1-18.

Cook, J. S., Kompfner, R., and Quate, C. F. (1956). "Coupled Helices,"
Bell System Tech. J. 35, 127-178.

Currie, M. R., and Forster, D. C. (1959). "A New Mechanism of Noise
Reduction in Electron Beams," J. Appl. Phys. 30, 94-103.

Currie, M. R., and Gould, R. W. (1960). "Coupled Cavity Traveling-
Wave Parametric Amplifiers-Part I," Proc. IRE 48, 1960-1973.

Forster, D. C. (1960). "Theory of Parametrically Pumped Longitudinal
Field Electron Beams," Report No. 14, Electron Tube and Microwave
Laboratory, California Institute of Technology, Pasadena, California.

Gould, R. W. (1955). "A Coupled Mode Description of the Backward Wave
Oscillator and the Kompfner Dip Condition," IRE Trans. on Electron
Devices ED-2, 37-42.

Hahn, W. C. (1939). "Small Signal Theory of Velocity Modulated Electron
Beams," Gen. Elec. Rev. 42, 258-270.

Harman, W. A. (1954). "Backward Wave Interaction in Helix Type Tubes,"
Report No. 13, Electron Devices Laboratory, Stanford University,
California.

Haus, H. A. (1958). "The Kinetic Power Theorem for Parametric Longitudinal Beam Amplifiers," IRE Trans. on Electron Devices ED-5, 225-232.

Haus, H. A., and Robinson, F. N. H. (1955). "The Minimum Noise Figure of Microwave Beam Amplifiers," Proc. IRE 43, 981-991.

Hutter, R. G. E. (1960). Beam and Wave Electronics in Microwave Tubes, D. Van Nostrand Co., New York.

Kino, G. S. (1953). "Some Data on the Sheath Helix with an External Shield," Internal Memorandum, Microwave Laboratory, Stanford University, California.

Kino, G. S. (1960). "A Parametric Amplifier Theory for Plasmas and Electron Beams," J. Appl. Phys. 31, 1449-1458.

Kompfner, R. (1946). "The Traveling Wave Valve-A New Amplifier for Centrimetric Wavelengths," Wireless World 52, 369-372.

Kompfner, R. (1950). "On the Operation of the Traveling Wave Tube at Low Level," British Jour. IRE 10, 283-289.

Llewellyn, F. B., and Peterson, L. C. (1944). "Vacuum Tube Networks," Proc. IRE 32, 144-166.

Louisell, W. H. (1955). "Analysis of the Single Tapered Mode Coupler," Bell System Tech. J. 34, 853-870.

Louisell, W. H. (1959). "A Three Frequency Electron Beam Parametric Amplifier and Frequency Converter," J. Electr. and Contr. VI, 1-25.

Louisell, W. H., and Quate, C. F. (1958). "Parametric Amplification of Space-Charge Waves," Proc. IRE 46, 707-716.

Manley, J. M., and Rowe, H. E. (1956). "Some General Properties of Nonlinear Elements-Part I," Proc. IRE 44, 904-913.

Monson, J. E. (1960). "Parametric Pumping of Space-Charge Waves," Report No. 317-1, Electron Devices Laboratory, Stanford University, California.

Mueller, W. M. (1960). "Propagation in Periodic Electron Beams," J. Appl. Phys. 32, 1349-1360.

Pierce, J. R. (1950). Traveling Wave Tubes, D. Van Nostrand Co., New York.

Pierce, J. R. (1954). "Coupling of Modes of Propagation," J. Appl. Phys. 25, 179-183.

Polovin, R. V. (1962). "Criteria for Instability and Gain," Soviet Phys.-Tech. Phys. 6, 889-895.

Putz, J. L., Luebke, W. R., Harman, W. W., and Spangenberg, K. (1952). "Operating Characteristics of a Folded Line Traveling-Wave Tube," Report No. 15, Electron Devices Laboratory, Stanford University, California.

Rack, A. J. (1938). "Effect of Space-Charge and Transit Time on the Shot Noise in Diodes," Bell System Tech. J. $\underline{17}$, 592-619.

Robinson, F. N. H. (1952). "Space-Charge Smoothing of Microwave Shot Noise in Electron Beams," Phil. Mag. $\underline{43}$, 51-62.

Schelkunoff, S. A. (1943). Electromagnetic Waves, D. Van Nostrand Co., New York.

Schottky, W. (1918). "Spontaneous Current Fluctuations in Electron Streams," Ann. Physik $\underline{57}$, 541-567.

Sensiper, S. (1955). "Electromagnetic Wave Propagation on Helical Structures," Proc. IRE $\underline{43}$, 149-161.

Siegman, A. E., Watkins, D. A., and Hsieh, H. C. (1957). "Density Function Calculations of Noise Propagation on an Accelerated Multi-Velocity Electron Beam," J. Appl. Phys. $\underline{28}$, 1138-1148.

Sturrock, P. A. (1958a). "A Variational Principle and an Energy Theorem for Small Amplitude Disturbances of Electron Beams and Electron-Ion Plasmas," Ann. Phys. $\underline{4}$, 306-324.

Sturrock, P. A. (1958b). "Kinematics of Growing Waves," Phys. Rev. $\underline{112}$, 1488-1503.

Sturrock, P. A. (1959). "Parametric Refrigeration-A Mechanism for the Removal of Noise from the Slow Wave of an Electron Stream," Report No. M. L. 656, Microwave Laboratory, Stanford University, California.

Sturrock, P. A. (1960a). "Action Transfer and Frequency Shift Relations in the Nonlinear Theory of Waves and Oscillations," Ann. Phys. $\underline{9}$, 422-434.

Sturrock, P. A. (1960b). "Excitation of Plasma Oscillations," Phys. Rev. $\underline{117}$, 1426-1429.

Sturrock, P. A. (1960c). "Parametric Refrigeration-A Mechanism for the Removal of Noise from the Slow Wave of an Electron Beam," Presented at the Fourth Intl. Congress on Microwave Tubes, Munich, Germany, June 1960. (Proceedings published by Academic Press, New York.)

Sturrock, P. A. (1960d). "Generalization of the Lagrange Expansion with Application to Physical Problems," J. Math. Phys. $\underline{1}$, 405-408.

Sturrock, P. A. (1960e). "In What Sense Do Slow Waves Carry Negative Energy," J. Appl. Phys. 31, 2052-2056.

Sturrock, P. A. (1961). "General Relations Concerning Multiply-Periodic Excitation of Nonlinear Dynamical Systems," Ann. Phys. 15, 250-265.

Tien, P. K. (1958). "Parametric Amplification and Frequency Mixing in Propagating Circuits," J. Appl. Phys. 29, 1347-1357.

Tien, P. K., Walker, L. R., and Wolontis, V. M. (1955). "A Large Signal Theory of Traveling-Wave Amplifiers," Proc. IRE 43, 260-277.

Varian, R. H., and Varian, S. F. (1939). "A High Frequency Oscillator and Amplifier," J. Appl. Phys. 10, 321-327.

Wada, G. (1956). "The Interdigital Line as a Backward Wave Structure," Report No. 384-1, Electron Devices Laboratory, Stanford University, California.

Wade, G. (1961). "Low Noise Amplifiers for Centimeter and Shorter Wave-Lengths," Proc. IRE 49, 880-891.

Wade, G., and Adler, R. (1959). "A New Method for Pumping a Fast Space-Charge Wave," Proc. IRE 47, 79-80.

Watkins, D. A. (1951). "Noise Reduction in Beam Type Amplifiers," Report No. 31, Electron Devices Laboratory, Stanford University, California.

Whinnery, J. R. (1954). "Noise Phenomena in the Region of the Potential Minimum," IRE Trans. on Electron Devices ED-1, 221-237.

White, R. M., Enderby, C. E., and Birdsall, C. K. (1963). "Properties of Ring-Plane Slow Wave Circuits," Report No. TIS-233-4, General Electric Microwave Laboratory, Palo Alto, California.

DISTRIBUTION LIST

CONTRACT NONR 225(48)

cc	Addresses	cc	Addresses

2 Chief of Naval Research
Department of the Navy
Washington 25, D. C.
Attention: Code 427

1 Commanding Officer
Office of Naval Research
1030 E. Green Street
Pasadena, California

1 Commanding Officer
Office of Naval Research
Branch Office
346 Broadway
New York 13, New York

Director
Naval Research Laboratory
Washington 25, D. C.
1 Attention: Code 3400
1   3600
1   3900
1   3930
1   1940

2 Chief, Bureau of Naval Weapons
Department of the Navy
Washington 25, D. C.
Attention: RREN

1 Director
Naval Electronics Laboratory
San Diego 52, California

10 ASTIA
Arlington Hall Station
Arlington 12, Virginia

1 Commanding Officer
Office of Naval Research
Branch Office
1000 Geary Street
San Francisco 9, California

1 Commanding Officer
Office of Naval Research
Branch Office
John Crerar Library Building
86 E. Randolph Street
Chicago 1, Illinois

10 Commanding Officer
Office of Naval Research
Navy 100
Fleet Post Office Box 39
New York, New York

2 Chief, Bureau of Ships
Navy Department
Washington 25, D. C.
Attention: Code 670

2 Chief, Bureau of Aeronautics
Navy Department
Washington 25, D. C.
Attention: Code AV

Chief, Naval Operations
Navy Department
Washington 25, D. C.
1 Attention: Code Op 30
1   Op 31

1 U. S. Naval Post Graduate School
Monterey, California

1 Commander
Naval Air Missile Test Center
Point Mugu, California

1 Chief, European Office
Air Research and Development Command
47 Rue Cantersteen
Brussels, Belgium

Commanding General
Air Force Research Division
Air Research and Development
    Command
Bedford, Massachusetts
8 Attention: CRRE
1   ERRSA-1

1 Director
Air University
Maxwell Air Force Base
Alabama
Attention: Cr 4582

1 Assistant Secretary of Defense
(Research and Development)
Department of Defense
Washington 25, D. C.
Attention: Technical Library

1 Chief, West Coast Office
USASRDL Building No. 6
75 South Grande Avenue
Pasadena 2, California

1 Chief Signal Officer
Department of the Navy
Washington 25, D. C.
Attention: SIGRD

1 Commanding Officer
U. S. Army Signal Missile
    Support agency
White Sands, New Mexico

1 Commanding General
U. S. Army Ordnance Missile
    Ground
Huntsville, Alabama
Attention: ORDAB-T

1 Commanding Officer
U. S. Naval Proving Ground
Dahlgren, Virginia

1 Commander
U. S. Naval Air Development
    Center
Johnsville, Pennsylvania

1 Commanding Officer
Office of Ordnance Research
Box CM, Duke Station
Durham, North Carolina

1 Airborne Instrument Laboratory
Comac Road
Deer Park, L. I., New York
Attention: John Dyer

1 U. S. Coast Guard
1300 E. Street, N. W.
Washington 25, D. C.
Attention: EEE

1 Secretary
Commission on Electrics
Office of the Assistant Secretary
    of Defense
(Research and Development)
Department of Defense
Washington 25, D. C.

1 Director of Army Research
Office, Chief of Research and
    Development
Washington 25, D. C.

1 Chief signal Officer
Department of the Army
Washington 25, D. C.
Attention: SIGCOO5b4

1 Commanding General
U. S. Army Electronic Proving
    Ground
Fort Huachuca, arizona
ATTN: Technical Library,
      Greely Hall

1 Commanding General
Naval Ordnance Laboratory
Corona, California

32 Signal Property Agent
Building 2504, Watson Area
Fort Monmouth, New Jersey
Attention: Officer of Research
        Operations

1	Bell Telephone Laboratories Murray Hill Laboratory Murray Hill, New Jersey Attention: Dr. J. R. Pierce	1	Commander Air Force Armanent Center Attention: Technical Library Elgin Air Force Base, Florida

1	Office of the Chief of
	    Engineers
	Department of the Army
	Washington 25, D. C.
		1	Commander
			Air Force Missile Development
			    Center
			Attention: Technical Library
			Holloman Air Force Base
			New Mexico

1	California Institute of
	    Technology
	Department of Electrical Eng.
	Pasadena, California
	Attention: Professor
	    L. M. Field
		1	Hq. U. S. Army Material Command
			Building T-7
			Attention: AMDRD-DE-MI
			Washington 4, D. C.

1	Commanding Officer Engineering Research and Development Laboratory Ft. Belvoir, Virginia	1	Commanding Officer Frankford Arsenal Bridesburg Philadelphia, Pennsylvania
1	Ballistics Research Laboratory Aberdeen Proving Ground Aberdeen, Maryland Attention: D. W. W. Delsasso		Commander Wright Air Development Division Wright-Patterson Air Force Base Ohio
2	Chief of Staff United States Air Force Washington 25, D. C. Attention: AFDRD-SC-3	2 4 1 1 1 1 2 1	Attention: WCLC WCLRC WCLRC WPLJ WCLJH WCRE WCRED WCRET
2	Commanding General Rome Air Development Center Griffiss Air Force Base Rome, New York Attention: RCRW	1	AEMTC (AEMTC Technical Library- MU 135) Patric Air Force Base Cocoa, Florida

5	Commander
	Air Force Office of Scientific
	    Research
	Attention: SRYA
	Washington 25, D. C.
		1	Chief, Physics Branch,
			    Division of Research
			U. S. Atomic Energy
			1901 Constitution Avenue, N. W.
			Washington 25, D. C.

1	National Science Foundation 1951 Constitution Avenue, N. W. Washington 25, D. C.		

1	Commander Arnold Engineering Development Center Attention: Technical Library Tullahome, Tennessee	1	Director Electronics Defense Group Engineering Research Institute University of Michigan Ann Arbor, Michigan
1	Commander Air Force Special Weapons Center Attention: Technical Library Kirtland Air Force Base New Mexico	1	Columbia University Columbia Radiation Laboratory New York 27, New York Attention: Mr. Bernstein
1	Commandant Air Force Institute of Tech. Attention: MCLI, Tech. Library Wright-Patterson Air Force Base Ohio	1	Cruft Laboratory Harvard University Cambridge, Massachusetts
		1	Dr. Winston H. Bostick Department of Physics Stevens Institute of Technology Hoboken, New Jersey
1	Commander Air Force Ballistic Missile Division Headquarters ARDC Attention: WDSQT Post Office Box 262 Inglewood, California	1	Sperry Gyroscope Company Great Neck, L. I., New York Attention: Technical Library
40	Stanford University Stanford, California	1	Sylvania Electric Systems Applied Research Laboratory 40 Sylvan Road Waltham 54, Massachusetts Attention: Charles E. Arnold
1	Sylvania Electric Products, Inc. 500 Evelyn Avenue Mountain View, California Attention: Special Tube Operations	1	Varian Associates 611 Hansen Way Palo Alto, California Attention: Technical Library
1	Ohio State University Department of Electrical Eng. Columbus 10, Ohio Attention: Professor E. M. Boone	1	University of Texas Defense research Laboratory Austin, Texas Attention: Harold D. Krick, Sr.

1	University of Michigan
	Willow Run Research Center
	Engineering Research Institue
	Ann Arbor, Michigan
	Attention: Dr. H. Goode
		1	Massachusetts Institute of
			  Technology
			Research Laboratory of
			  Electronics
			Cambridge 39, Massachusetts
			Attention: Mr. Hewitt
			   Librarian

1 Brooklyn Polytechnic Institute
Microwave Research Institute
55 Johnson Street
Brooklyn 1, New Jersey
Attention: Mr. Jerome Fox

1 Dr. John R. Whinnery
Division of Electrical Eng.
University of California
Berkeley 4, California

1 Professor Hans Motz
Oxford University
Oxford, England

1 Lincoln Laboratory
Massachusetts Institute of
Technology
P O. Box 73
Lexington, Massachusetts

1 Gilfillian Brothers
1815 Venice Blvd.
Los Angeles, California
Attention: Countermeasures
Laboratories

1 Hallicrafters
4401 West 5th Street
Chicago, Illinois
Attention: William Frankart

1 The Maxson Corporation
460 West 34th Street
New York 1, New York

1 Motorola, Incorporated
8330 Indiana Avenue
Riverside, California
Attention: Robert W. Barton

1 Raytheon Manufacturing Corp.
Waltham 54, Massachusetts
Attention: Research Division
Library

1 Sperry Gyroscope Company
Electronic Tube Division
Great Neck, L. I., New York
Attention: T. Sege

4 Office of Ordnance
U. S. Army
Box CM, Duke Station
Durham, North Carolina

1 Electron Tube Division of the
Research Laboratory
General Electric Company
The Knolls
Schenectady, New York

1 Glenn L. Martin Company
Baltimore, Maryland
Attention: Mary E. Exxo

1 Hughes Aircraft Company
Florence Ave. and Teale St.
Culver City, California
Attention: Mr. Nicholas E. Devereux
Technical Document Center

1 The Rand Corporation
1700 Main Street
Santa Monica, California
Attention: Margaret Anderson
Librarian

1 Dr. Walter Higa
Engineering Specialist
Research Group Supervisor
California Institute of Technology
4800 Oak Grove Drive
Pasadena 3, California

1 General Electric Microwave Lab.
601 California Avenue
Palo Alto, California
Attention: Librarian

1 Pacific Union College
Physics Department
Angwin, California
Attention: Dr. Ivan Neilson

1   Dr. A. D. Berk
    4134 Del Rey Avenue
    Venice, California

1   Dr. A. F. Pierce
    Imperial College of Science
        and Technology
    South Kensington
    London, S. W., England

1   The Mitre Corporation
    P. O. Box 208
    Lexington 73, Massachusetts

1   Mr. Jack Summers
    Varian Associates
    611 Hansen Way
    Palo Alto, California

1   General Electric Company
    Power Tube Division
    Electronic Components Division
    Building 269, Room 205
    One River Road
    Schenectady 5, New York

1   Litton Industries
    Electron Tube Division
    960 Industrial Road
    San Carlos, California

1   Eitel-McCullough, Inc.
    Research Library
    301 Industrial Way
    San Carlos, California

1   Stanford Research Institute
    Menlo Park, California
    Attention: Documents Center

1   Bendix Corporation
    Red Bank Division
    Eatontown, New Jersey
    Attention: Mr. S. Barbasso

1   High-Power Klystron Department
        G.38
    Attention: Dr. John Romaine
    Sperry Gyroscope Company
    Great Neck, L. I., New York

1   Dr. Bertil Agdur
    Microwave Department
    Royal Institute of Technology
    Stockholm, Sweden

1   California Institute of Technology
    Electron Tube Laboratory
    Pasadena, California

1   Robert Vehn
    Watkins-Johnson Company
    3333 Hillview Avenue
    Palo Alto, California

1   Sperry Electronic Tube Division
    Sperry Rand Corporation
    Gainesville, Florida

1   Research Division Library
    Raytheon Company
    28 Seyon Street
    Waltham 54, Massachusetts

1   Mr. J. F. Kane
    Kane Engineering Laboratories
    845 Commercial Street
    Palo Alto, California

1   Phillips Laboratories
    Division of North American
        Phillips Company, Inc.
    Irvington-on-Hudson
    New York
    Attention: Robert C. Bohlinger

1   Director
    U. S. Naval Research Labs.
    Washington 25, D. C.
    Attention: Code 5300

1　Sperry Phoenix Company
　　Division of Sperry Rand Corp.
　　Phoenix, Arizona
　　Attention: Tech. Librarian

1　TUCOR, Incorporated
　　18 Marshall Street
　　South Norwalk, Connecticut
　　Attention: Mrs. Marion Osband

1　Professor H. W. Konig
　　Institute fur
　　　　Hochfrequenztechnik
　　Technische Hochschule
　　Vienna 4, Gusshausstrasse 25
　　Austria

1　Dr. V. L. Stout, Manager
　　Physical Electronic Research
　　P. O. Box 1088
　　Schenectady, New York

1　Institute for Defense Analysis
　　Research and Engineering
　　Support Division
　　1825 Connecticut Ave. N.W.
　　Washington 25, D. C.
　　Attn: Technical Information
　　　　　Office

1　Director
　　National Security Agency
　　Fort George G. Meade, Maryland
　　Attention: CREF-332 (Rm. 2C087)
　　　　　　　　Miss Creswell
　　　　　　　　Librarian

1　Research Center for the Airtron
　　Division of Litton Industries
　　200 East Hanover Avenue
　　Morris Plains, New Jersey
　　Attn: J. W. Neilson, Manager
　　　　　Solid State Materials
　　　　　Laboratory

1　Commanding Officer
　　U. S. Army Research Office
　　　Durham
　　Box CM, Duke Station
　　Durham, North Carolina
　　Attn: CRD-AA-IP, Mr. Ulsh

1　Cornell University
　　School of Electrical Engineering
　　Ithaca, New York
　　Attn: Professor G. C. Dalman

1　Carlyle Barton Lab.
　　The John Hopkins University
　　Charles and 34th Streets
　　Baltimore 18, Maryland
　　Attn: Librarian

1　Professor Sanai Mito
　　Osaka City University
　　Department of Engineering
　　12 Nishi-Ogimachi, Kitaku
　　Osaka, Japan

1　CERN
　　Service d'Information Scientifique
　　Attn: Mme L. Goldschmit-Clermont
　　Geneva 23, Switzerland

1　Amphenol-Borg Electronics
　　　Corporation
　　2801 South 25th Avenue
　　Broadview, Illinois
　　ATTN: Mr. R. C. Becker
　　　　　　Senior Staff Engineer

1　Mr. Glen Wade
　　Spencer Laboratories
　　Burlington, Massachusetts

1　Scientific Attache
　　Swedish Embassy
　　2249 R. Street, N. W.
　　Washington 8, D. C.

1   Dr. Yen
    Department of Electrical Eng.
    University of Toronto
    Toronto 5, Ontario
    Canada

1   M. A. Allen
    Microwave Associates, Inc.
    Burlington, Massachusetts

3   Commanding Officer
    U. S. Army Research Office
       Durham
    Attn: CRD-AA-IP, Box CM
    Duke Station
    Durham, North Carolina

1   Raytheon Company
    Research Division
    Waltham 54, Massachusetts
    Attn: Mrs. Madaleine Benett
           Librarian

1   USNPG
    Monterey, California
    Attn: Professor Gray
    Electronics Department

1   Dr. E. A. Ash
    Standard Telecommunications Lab,
       Ltd.
    London Road
    Harlow, Essex
    England

1   Dr. W. Veith
    Siemens and Halske Aktiengesell-
       schaft
    St. Martin Strasse 76
    Munchen 8, Germany

1   Dr. Humio Inaba
    Electrical Engineering Dept.
    Tohoku University
    Sensai, Japan

1   Dr. T. Rossing
    St. Olaf College
    Northfield, Minnesota

1   Carnegie Institute of Technology
    Dept. of Electrical Engineering
    Schenley Park
    Pittsburgh 13, Penn.

1   U. S. Atomic Energy Commission
    Research Division
    Washington 25, D. C.
    Attn: Mr. Wm. C. Gough